THE ASTROPHYSICAL JOURNAL, 417:220–242, 1993 November 1

COLLAPSE OF MAGNETIZED MOLECULAR CLOUD CORES. I. SEMIANALYTICAL SOLUTION

DANIELE GALLI[1] AND FRANK H. SHU[2]
Department of Astronomy, University of California at Berkeley
Received 1993 January 25; accepted 1993 May 10

ABSTRACT

In this paper we follow the evolution of an unstable magnetized cloud core modeled with the density distribution of a singular isothermal sphere and threaded by a uniform magnetic field. We include neutral-ion slip, and we solve the equations by an expansion about the known self-similar problem without magnetism. We find that the magnetic field does not significantly modify the standard rate of mass infall because of two offsetting effects: the Lorentz force that impedes gravitational collapse, and the increased characteristic speed that causes the initiation of infall to travel outward faster (as a fast magnetohydrodynamic wave rather than an acoustic wave). Strong magnetic pinching forces deflect infalling gas toward the equatorial plane to form a flattened disequilibrium structure ("pseudodisk") around the central protostar. The perturbative approach allows us to calculate analytically the dependence of the radius of the pseudodisk at small times on the physical parameters of the problem when a dimensionless coefficient of order unity is supplied by a separate numerical calculation for the nonlinear flow in the inner region (Paper II).

Subject headings: ISM: clouds — ISM: magnetic fields — ISM: molecules — MHD — stars: formation

1. INTRODUCTION

1.1. *Motivation and Previous Work*

Magnetic fields play an important dynamical role in regions of star formation (see McKee et al. 1993 and Heiles et al. 1993 for recent reviews of the theoretical results and the observational data, respectively). A large body of theoretical work has been devoted to the structure of *equilibrium* configurations and to the *quasi-static* evolution of magnetic, self-gravitating molecular clouds (e.g., see Mouschovias 1976a, b; Nakano 1979, 1984, 1988; Paleologou & Mouschovias 1983; Shu 1983; Tomisaka, Ikeuchi, & Nakamura 1988a, b, 1989, 1990; Tomisaka 1991; Lizano & Shu 1989, hereafter LS). Because of the greater complexity of a dynamical calculation in comparison to a static or quasi-static one, studies of the *collapse* of magnetic molecular clouds, even in the simplest idealizations, have been based almost exclusively on numerical simulations. Scott & Black (1980) performed the first numerical analysis of the dynamical evolution of an initially spherical, nonrotating, axisymmetric, molecular cloud with a frozen-in magnetic field. Black & Scott (1982) later used the same code to study the drift of plasma and magnetic field relative to the neutral gas (i.e., ambipolar diffusion; see also El-Nawawy, Aiad, & El-Shalaby 1988 for the effects of ohmic dissipation). Under the assumption of field-freezing, Dorfi (1982) executed fully three-dimensional simulations of the dynamics of rotating, magnetic, and self-gravitating clouds to investigate the processes of magnetic braking and fragmentation (see also Phillips & Monaghan 1985 and Phillips 1986a, b for a method based on "smoothed particle hydrodynamics").[3]

Despite the differences in the emphasis given to the relevant physical processes, the situation envisaged in all the above numerical simulations is that of a molecular cloud having an initially supercritical mass-to-flux ratio and therefore collapsing *as a whole* and, possibly, fragmenting. From a theoretical standpoint, both supercritical and subcritical initial conditions are of interest (Mestel 1965, 1985). In particular, differences in the initial conditions may provide a natural explanation for the occurrence of two distinct modes of star formation: in compact groups and in relative isolation (Shu, Adams, & Lizano 1987; LS; cf. Mouschovias 1987a, b).

Recent observations show that clumps within molecular clouds, with the possible exception of the most massive ones, are typically subcritical (Carr 1987; Loren 1989; see also examples and discussion in Heiles et al. 1993). For subcritical clumps that remain magnetically supported in the large, one wishes to follow the quasi-static process of the localized formation of dense cores by ambipolar diffusion until the attainment of a critical or supercritical mass-to-flux ratio in its central regions, and to determine the characteristics of the subsequent dynamical collapse. In a series of publications of increasing geometrical sophistication (slab to infinite cylinder to three-dimensional figure with axial symmetry), Mouschovias and coworkers (Mouschovias, Paleologou, & Fiedler 1985; Mouschovias & Morton 1991, 1992a, b; Fiedler & Mouschovias 1992) have used adaptive-mesh techniques to address the problem of the transition from quasi-static contraction to dynamical collapse. Continued gravitational collapse, however, cannot be sustained in an isothermal slab or infinite cylinder that has an accessible equilibrium state (e.g., see Spitzer 1968); thus, we must view with caution the claim by Mouschovias & Morton (1992b) that mass infall rates are magnetically controlled in all geometries (i.e., limited by ambipolar-diffusion rather than dynamical time scales).

[1] Postal address: Osservatorio Astrofisico di Arcetri, Largo E. Fermi, I-50125 Firenze, Italy.
[2] Postal address: Department of Astronomy, 601 Campbell Hall, University of California, Berkeley, CA 94720.
[3] Dudurov and coworkers (see Dudurov 1988, 1990 and references therein) followed numerically the evolution of the magnetic flux of a collapsing cloud in the kinematic approximation and in one-dimensional spherical geometry, including both ambipolar and ohmic diffusion; unfortunately, their results are in large part unavailable in English translation.

The boundary conditions used by numerical simulations imply that matter and magnetic flux cannot enter or exit through the boundaries. This requirement would not cause any worry if the computational volume contained substantially more material than needed to form the final collapse object (as real molecular clouds seem to do), but practical constraints typically prevent such large grids. In the formulation given below, we circumvent this restriction by not introducing an artificially imposed size to the original cloud "core."

1.2. *The Case of Isolated Low-Mass Star Formation*

The case of the formation of isolated low-mass stars offers the special advantage that the theoretical framework is fairly well developed and in substantial agreement with the observations (see the reviews of Shu et al. 1987, 1993; Evans 1991; Lada 1991). According to this picture, small dense cores condense inside a molecular cloud by gradually losing magnetic (and turbulent) support via the process of ambipolar diffusion, as originally proposed by Mestel and Spitzer (1956) (stage 1); the cores then approach a state resembling a singular isothermal sphere, and, if they pass the brink of instability, they ultimately collapse from inside-out (Shu 1977), building up a central protostar and a nebular disk surrounded by an infalling envelope of gas and dust (stage 2); a stellar or disk wind then emerges from the rotational poles of the system, producing a bipolar flow that reverses the infall (stage 3), eventually revealing an optically visible star surrounded by a centrifugally supported circumstellar disk (stage 4).

This description offers the advantage that the gravitational collapse of a singular isothermal sphere (stage 2) possesses a self-similar solution (taking the form of a spherical expansion wave propagating outward at the sound speed) that can be found semianalytically, thereby providing a convenient starting point for further analysis and refinement. Moreover, Zhou et al. (1990, 1992) and Zhou (1992) have shown that the inside-out collapse solution provides a much better interpretation of molecular lines profiles observed in isolated molecular cloud cores and Bok globules than alternative theoretical models. On the other hand, the original formulation by Shu (1977) contained a number of oversimplifications, the most serious ones being the neglect of rotation and magnetic fields in the initial configuration.

The effects of rotation were considered by Terebey, Shu, & Cassen (1984, hereafter TSC) as a perturbation to the nonrotating solution. A number of authors (e.g., Adams & Shu 1986; Adams, Lada, & Shu 1987, 1988; Butner et al. 1991; Natta et al. 1992; Whitney & Hartmann 1992) have used the TSC solution as the dynamical basis for radiative-transfer computations of the emergent spectral energy distributions or scattered polarized radiation expected from rotating protostars. These models yield reasonable agreement with the available observational data for embedded infrared sources, bipolar flow sources, and biconical reflection nebulae, but the angular rotation rates Ω of the original cloud cores needed to obtain good fits often appear uncomfortably large in comparison with the observational measurements or limits of detection (e.g., see Myers et al. 1991). The present work demonstrates that the inclusion of magnetic fields of reasonable strength can serve an equivalent purpose of flattening and emptying-out of the central density contours; thus, the empirical values of Ω derived from previous model studies need to be lowered in light of this modification.

2. THE PROBLEM AND THE PHYSICAL SCALES

2.1. *The Method and the Choice of the Initial State*

Among others, LS have formulated and solved the problem of the quasi-static condensation of a dense core from a diffuse background by ambipolar diffusion, including a semiempirical treatment of turbulent pressure. Figure 1 summarizes the basic features of the phase of quasi-static evolution of a molecular cloud core according to their calculations, for the case where turbulent pressure is relatively unimportant (their model $K = 6$). In a cylindrical coordinate system (R, φ, z), the panels show the density profile along the R- and z-axes, the differential mass-to-flux ratio $dM/d\Phi(R)$ (for a flux tube which crosses the equatorial plane at radius R), and the ratio of magnetic to thermal pressure $\alpha(R)$ along equatorial radius at three different times ($t = 0$, 0.21, and 0.23, in LS's units).

Toward the end of the phase of quasi-static contraction, molecular cloud cores tend to acquire the density profile of a modified singular isothermal sphere (see LS; Tomisaka et al. 1988b; and the discussion in Shu et al. 1993, § 3), in a spherical coordinate system (r, θ, φ)

$$\rho(r, \theta) = \frac{a^2}{2\pi G r^2} Q(\theta) , \tag{1}$$

where a is the effective isothermal sound speed (including the effects of an isotropic turbulent pressure) and $Q(\theta)$ is a nondimensional shape function (equal to unity when averaged over all solid angles), that accounts for the anisotropy of magnetic forces. In particular, if $Q(\theta) = 1$, the mass contained in a cylinder of radius R about the z-axis reads

$$M(R) = \frac{\pi a^2}{G} R . \tag{2}$$

LS showed that a small compression of the magnetic field threading a core, followed by gas flow along field lines, produces a considerable enhancement of the central density, since ambipolar diffusion "drags out" field lines relative to the neutral gas, forcing the large-scale (poloidal) magnetic field to remain *nearly* straight and uniform. Since the magnetic flux of an uniform magnetic field of strength B_0 in the z-direction is

$$\Phi(R) = \pi B_0 R^2 , \tag{3}$$

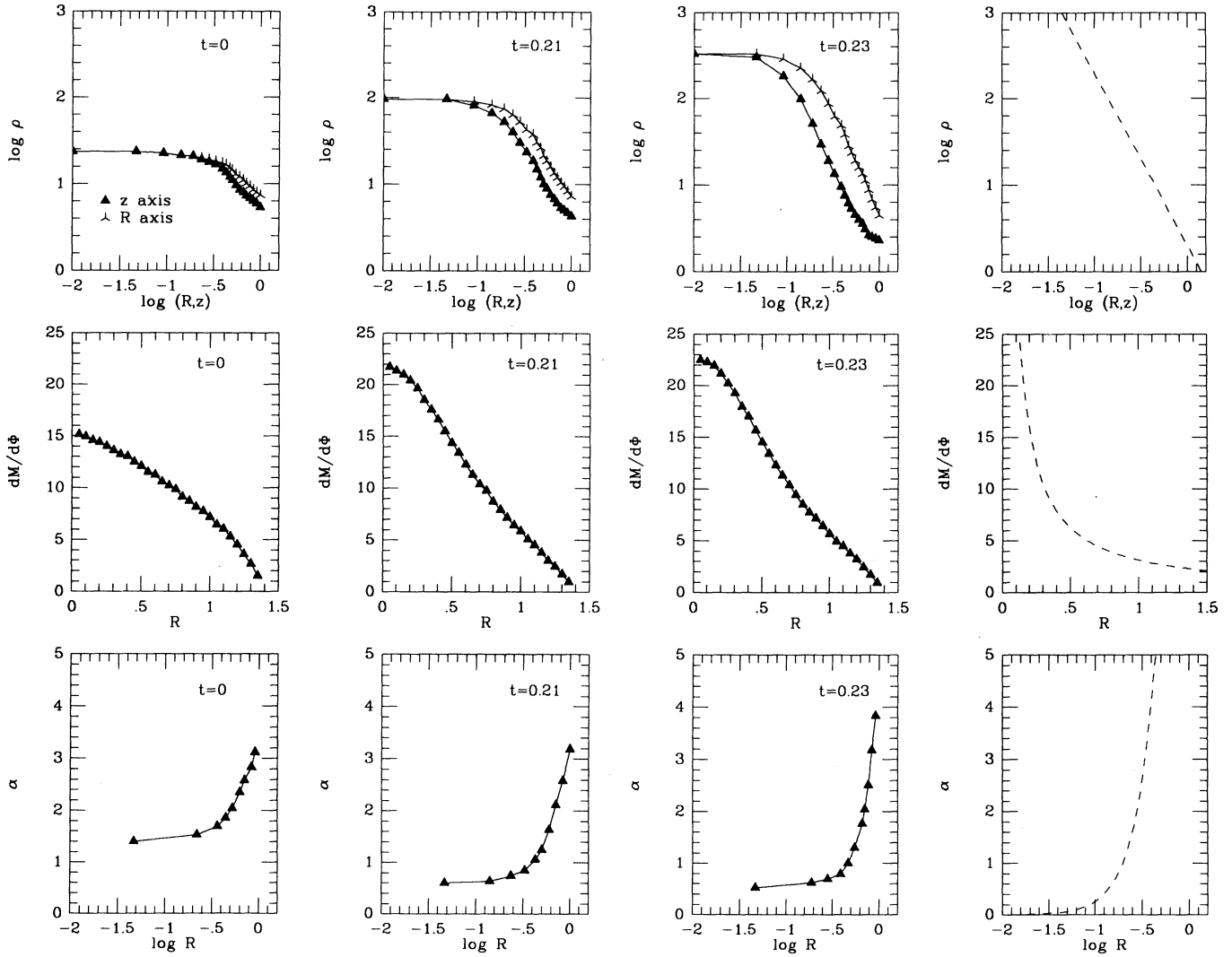

FIG. 1.—Formation of a molecular cloud core by ambipolar diffusion, according to the calculations of LS (their case $K = 6$). The panels show the evolution of density, differential mass-to-flux ratio and ratio of magnetic to thermal energy α as function of the cylindrical coordinates (R, z) at three different times: $t = 0$, 0.21, and 0.23. All physical quantities are expressed in the units of LS: numerically, the unit of time is 6×10^6 yr, the unit of length is 0.11 pc, the unit of density is $10^3 m_H$ cm^{-3}, and the unit of the mass-to-flux ratio is 0.38 $M_\odot$ μG^{-1} pc^{-2}. Panels in the last column show the same quantities in the same units for the singular isothermal sphere threaded by a uniform magnetic field, as described by eq. (1), with $Q(\theta) = 1$, and eq. (3).

the mass-to-flux ratio and the differential mass-to-flux ratio for a singular isothermal sphere threaded by an uniform magnetic field read, from equation (2) and (3),

$$\frac{M}{\Phi}(R) = \frac{a^2}{B_0 G}\frac{1}{R} \tag{4}$$

and

$$\frac{dM}{d\Phi}(R) = \frac{a^2}{2B_0 G}\frac{1}{R}, \tag{5}$$

respectively. The ratio of magnetic to thermal pressure for the same configuration is

$$\alpha(R) = \frac{B_0^2 G}{4a^4} R^2 . \tag{6}$$

The last column of panels in Figure 1 shows the density profile given by equation (1) with $Q(\theta) = 1$ and the quantities $dM/d\Phi(R)$ and $\alpha(R)$, given by equations (5) and (6), in the same units as LS.

The models of LS exhibit a "bimodal opposition to gravity" (Mouschovias 1991a, b), wherein thermal pressure forces dominate in the dense central region (core), and magnetic and turbulent forces dominate in the rarefied outer part (envelope). The smallness of

α in the part of the cloud destined to form a protostar motivates the present perturbative study of the collapse of the unstable equilibrium states described by equations (1) with $Q(\theta) = 1$ and (3). In this analysis we treat magnetic effects (initially) as a small correction to the exact self-similar solution of Shu (1977) for the collapse of a singular isothermal sphere (see § 3).

Figures 2, 3, and 5 of LS show that realistic configurations become gravitationally unstable in their central regions before a singularity develops, that the magnetic field lines at that instant are not perfectly and uniform, and that the density contours are aspherical, that is, $Q(\theta) \neq 1$. Nevertheless, in the inner regions the initial oblateness is small and easily overwhelmed by the dynamical flattening introduced by magnetic forces during the collapse (see § 5 and Paper II). Moreover, the choice of an uniform and straight magnetic field appropriately mimics the tendency of ambipolar diffusion to produce centrally condensed density distributions without a corresponding large increase in the magnetic field strength. In the case $K = 6$ considered by LS, when the available means of support in the cloud can no longer prevent the collapse of the inner region (at $t = 0.23$), the field strength at the center of the cloud core exceeds the value at the surface ("tidal lobe") only by a factor ~ 2.5; the corresponding density contrast measures ~ 100. The subsequent evolution should therefore resemble the dynamical collapse of the equilibrium state described by equations (1) and (3).

2.2. *Fundamental Physical Quantities*

Consider then the density profile given by equation (1) with $Q(\theta) = 1$:

$$\rho(r) = \frac{a^2}{2\pi G r^2} . \tag{7}$$

The only dimensional parameters that enter in any description of the dynamical evolution of such a configuration are the gravitational constant G and the effective sound speed a. As defined above, a provides more a measure of the proportionality constant in the power-law density distribution than the thermal sound speed; therefore it can include, in principle, the effects of turbulent magnetic fields or wavelike motions that help to support the cloud core against its self-gravity. From the impossibility of constructing a characteristic length scale from G and a only, if follows that the gravitational collapse of a nonmagnetic singular isothermal sphere possesses a self-similar solution (Shu 1977).

Since we wish to focus on the effects of an ordered magnetic field B_0, we do not consider here the effects of rotation at an initial solid-body rate Ω. On an intermediate scale, the effects of rotation and magnetic field are both small, and the perturbative solutions of TSC and this paper may simply be added linearly. For the inner problem, we shall find that magnetic effects amplify typically more quickly than centrifugal effects, so the buildup of centrifugally supported disks may occur more through equatorial feeding from a larger pseudodisk than from infall directly from the molecular cloud core (see Paper II). In any case, the introduction of the dimensional quantity B_0 by itself breaks the exact self-similarity of the problem. The only combination of G, a, and B_0 having the dimension of length is $a^2 B_0^{-1} G^{-1/2}$ (see Appendix A). Defining

$$r_m = \frac{2a^2}{B_0 \sqrt{G}} , \tag{8}$$

we see from equation (6) that at $R = r_m$ magnetic pressure equals thermal pressure in the initial state, $\alpha(R = r_m) = 1$. From equation (4) we obtain $M/\Phi(R = r_m) = 1/2\sqrt{G}$, which is larger than the critical value given by $(M/\Phi)_{cr} = c/\sqrt{G}$, where $c \simeq 0.12$–0.13 (Mestel 1965; Mouschovias & Spitzer 1976; Tomisaka et al. 1988a, b; see also McKee et al. 1993 and references therein); therefore, the mass contained in a flux tube of radius $R = r_m$ is initially in a state of unstable equilibrium under the balance of gravity and thermal pressure and cannot be supported during its collapse by magnetic forces even if the field remains frozen in the fluid. Considered on a spatial scale larger than $r_{cr} = r_m/2c \simeq 4r_m$; however, the cloud is magnetically subcritical.

We find it informative to estimate the numerical value of r_m, as defined above, for typical molecular cloud cores. Throughout this paper we will adopt the reference values $a = 0.35$ km s^{-1} for the effective sound speed and $B_0 = 30$ μG for the initial uniform magnetic field. The length scale r_m then reads

$$r_m = 3.16 \times 10^{17} \left(\frac{a}{0.35 \text{ km s}^{-1}}\right)^2 \left(\frac{B_0}{30 \ \mu\text{G}}\right)^{-1} \text{cm} , \tag{9}$$

and the corresponding crossing time for an acoustic disturbance is

$$t_m = \frac{r_m}{a} = 9.03 \times 10^{12} \left(\frac{a}{0.35 \text{ km s}^{-1}}\right) \left(\frac{B_0}{30 \ \mu\text{G}}\right)^{-1} \text{s} , \tag{10}$$

or about 2.9×10^5 yr for the standard values of the parameters. From equation (2) the mass contained in a cylindrical flux tube of radius $R = r_m$ equals

$$M(R = r_m) \simeq 9 \left(\frac{a}{0.35 \text{ km s}^{-1}}\right)^4 \left(\frac{B_0}{30 \ \mu\text{G}}\right)^{-1} M_\odot , \tag{11}$$

whereas the mass contained in a sphere of the same radius is smaller by a factor $\pi/2$. The corresponding values inside $R = r_{cr}$ are larger by a factor 4.

3. THE GOVERNING EQUATIONS

3.1. *The Magnetohydrodynamic Equations*

Under typical molecular cloud conditions, a gas consisting of electrons (e), ions (i) of charge $+Ze$, and neutrals (n) behaves with excellent approximation as a two-fluid system (if we ignore charged grains altogether). The small electric currents required to maintain a large-scale interstellar magnetic field of typical strength imply a negligible ion-electron velocity drift

$$\boldsymbol{u}_e \simeq \boldsymbol{u}_i \,, \tag{12}$$

whereas the condition of charge neutrality requires

$$\rho_e = \rho_i \frac{Zm_e}{m_i} \,; \tag{13}$$

therefore, we may eliminate from consideration separate dynamical equations for the electrons. In addition, the contribution of the ions to the total gas density is negligible (typically $\rho_i \ll \rho_n$ by about six orders of magnitude in molecular clouds). For numerical estimates we adopt for the mass of the average neutral particle $m_n = 2.3 m_{\rm H}$ and for the average ion $m_i = 30\, m_{\rm H}$, where $m_{\rm H}$ is the mass of the hydrogen atom (e.g., see Nakano 1984).

Over a wide range of cloud conditions, ion-neutral drift provides the dominant mechanism for field diffusion (e.g., see Umebayashi & Nakano 1990). If we leave aside the issue of ohmic dissipation for a later discussion, the magnetohydrodynamic (MHD) equations take the following form:

(a) the equation of continuity

$$\frac{\partial \rho_n}{\partial t} + \nabla \cdot (\rho_n \boldsymbol{u}_n) = 0 \,, \tag{14}$$

(b) the equation of motion for the neutrals

$$\rho_n \left[\frac{\partial \boldsymbol{u}_n}{\partial t} + (\boldsymbol{u}_n \cdot \nabla) \boldsymbol{u}_n \right] = -a^2 \nabla \rho_n - \rho_n \nabla V + \gamma \rho_n \rho_i (\boldsymbol{u}_i - \boldsymbol{u}_n) \,, \tag{15}$$

(c) the Poisson equation

$$\nabla^2 V = 4\pi G \rho_n \,, \tag{16}$$

(d) the induction equation

$$\frac{\partial \boldsymbol{B}}{\partial t} = \nabla \times (\boldsymbol{u}_i \times \boldsymbol{B}) \,, \tag{17}$$

and (e) the condition of no monopoles

$$\nabla \cdot \boldsymbol{B} = 0 \,. \tag{18}$$

The symbols in the above equations have their usual meanings; the term proportional to the ion-neutral velocity drift in equation (15) represents the mean drag force on the neutrals (per unit volume) associated with momentum exchange in ion-neutral collisions, and γ is the drag coefficient, $\gamma = 3.5 \times 10^{13}$ cm^3 g^{-1} s^{-1} (Draine, Roberge, & Dalgarno 1983).

If we neglect inertial, gravitational, and pressure forces (all proportional to ρ_i) compared to the Lorentz force on the ions because of the low ionization fraction, the equation of motion for the ions reads

$$\gamma \rho_n \rho_i (\boldsymbol{u}_i - \boldsymbol{u}_n) = \frac{1}{4\pi} (\nabla \times \boldsymbol{B}) \times \boldsymbol{B} \,, \tag{19}$$

and the velocity of the ions can be obtained algebraically once the velocity of the neutrals and the magnetic field have been determined. Hence, if the density of the ions can be specified in terms of the density of the neutrals (see § 3.2), the solution of the equations for the neutral component and the magnetic field completely determines the solution of the problem.

The diffusion of magnetic field associated with the ion-neutral drift is made explicit by using equation (19) to eliminate the velocity of the ions from the induction equation:

$$\frac{\partial \boldsymbol{B}}{\partial t} + \nabla \times (\boldsymbol{B} \times \boldsymbol{u}_n) = \nabla \times \left\{ \frac{\boldsymbol{B} \times [\boldsymbol{B} \times (\nabla \times \boldsymbol{B})]}{4\pi \gamma \rho_n \rho_i} \right\} . \tag{20}$$

The term on the right-hand side then represents the effect of ambipolar diffusion.

We may simplify the induction equation further by assuming that the configuration is axisymmetric and that $\boldsymbol{B}$ is purely poloidal. Since $\boldsymbol{B}$ is solenoidal, in spherical coordinates (r, θ, φ) we find it convenient to introduce a vector potential $\boldsymbol{A}$ in the $\hat{\boldsymbol{e}}_\varphi$ direction,

$$\boldsymbol{A}(r, \theta, t) = \frac{\Phi(r, \theta, t)}{2\pi r \sin \theta} \hat{\boldsymbol{e}}_\varphi \,, \tag{21}$$

where $\Phi(r, \theta, t)$ is the *magnetic flux function* (reducing to eq. [3] in the particular case of an uniform magnetic field). We may express a poloidal magnetic field in terms of Φ as

$$\boldsymbol{B} = \nabla \times \boldsymbol{A} = \frac{1}{2\pi r \sin\theta}\left[\frac{1}{r}\frac{\partial\Phi}{\partial\theta}\hat{\boldsymbol{e}}_r - \frac{\partial\Phi}{\partial r}\hat{\boldsymbol{e}}_\theta\right], \tag{22}$$

and write the induction equation (20) in the scalar form,

$$\frac{\partial\Phi}{\partial t} + \boldsymbol{u}_n \nabla\Phi = \frac{1}{16\pi^3\gamma\rho_n\rho_i}\left(\frac{\partial^2\Phi}{\partial r^2} + \frac{1}{r^2}\frac{\partial^2\Phi}{\partial\theta^2} - \frac{\cot\theta}{r^2}\frac{\partial\Phi}{\partial\theta}\right)\frac{|\nabla\Phi|^2}{r^2\sin^2\theta}. \tag{23}$$

3.2. *Ionization Equilibrium*

To close the system of MHD equations, we need a relation between the ion and the neutral density. Whereas current observations (Langer 1985; Falgarone & Pérault 1987) do not allow precise determinations of the ionization fraction in molecular clouds, detailed computations of ionization-recombination equilibria have been performed by a number of authors (Dalgarno, Oppenheimer, & Berry 1973; Oppenheimer & Dalgarno 1974; Nakano 1976; Elmegreen 1979; Nakano 1979; Umebayashi & Nakano 1980; Umebayashi 1983; Nakano 1984; Nakano & Umebayashi 1986; Umebayashi & Nakano 1990; Nishi, Nakano, & Umebayashi 1991; Nakano 1992; El-Nawawy, Ateya, & Aiad 1992). At the most basic level, when ionization by cosmic rays (at a rate ζn_n, with $\zeta \sim 10^{-17}$ s^{-1}) is balanced by dissociative recombination (at a rate $\beta n_e n_i$, with $\beta \sim 10^{-6}$ cm^3 s^{-1}), we obtain a power-law expression for the density of ions

$$\rho_i = C\rho_n^k, \tag{24}$$

with $C = (m_i^2\zeta/\beta m_n)^{1/2} \sim 10^{-16}$ g$^{1/2}$ cm$^{-3/2}$ and $k = \frac{1}{2}$.

Results from the detailed models quoted above generally agree with this rough estimate, with C depending weakly on the gas temperature and more strongly on the ambient metal depletion. For instance, over the density range 10^4 cm$^{-3} < n < 10^{11}$ cm^{-3}, Figures 1 from Elmegreen (1979) and Nakano (1981) both imply $C = 3 \times 10^{-16}$ g$^{1/2}$ cm$^{-3/2}$ and $k = \frac{1}{2}$, whereas Figure 2 from Umebayashi & Nakano (1990) gives $k = \frac{1}{2}$ and a significantly smaller coefficient, $C = 3 \times 10^{-17}$ g$^{1/2}$ cm$^{-3/2}$ for depleted dense molecular clouds. We adopt for fiducial purposes the "canonical" values of Elmegreen (1979) and Nakano (1981), but we note that a smaller value of C would lead to less strong coupling of the magnetic field with the gas.

The assumption of ionization-recombination equilibrium in a problem involving dynamical collapse holds since the time scale for ionization-recombination (of the order of $n_e/\zeta n_n$) is much shorter than the dynamical (free-fall) time scale of the cloud over the entire range of densities of interest here (see, e.g., Umebayashi & Nakano 1990). In principle, near the central source we should also consider the effects of thermo- and photo-ionization. At the scales of interest here (typically $>10^2$ AU), however, we may ignore such complications for the problem of low-mass star formation.

3.3. *Similarity Variables*

Motivated by the studies of Shu (1977) and TSC, we introduce the similarity variables

$$\boldsymbol{x} = \frac{\boldsymbol{r}}{at} \quad \text{and} \quad \tau = \frac{t}{t_m}, \tag{25}$$

in terms of which the time and space derivatives are expressed as

$$\left(\frac{\partial}{\partial t}\right)_r = \frac{1}{t_m}\left[\left(\frac{\partial}{\partial\tau}\right)_x - \frac{1}{\tau}(\boldsymbol{x}\cdot\nabla_x)_\tau\right], \tag{26}$$

$$(\nabla_r)_t = \frac{1}{at_m\tau}(\nabla_x)_\tau. \tag{27}$$

We now define the nondimensional density of the neutrals α_n, velocities $\boldsymbol{v}_{i,n}$, gravitational potential ψ, magnetic field $\boldsymbol{b}$, magnetic flux ϕ, and mass m interior to radius x by

$$\rho_n(\boldsymbol{r}, t) = \frac{1}{4\pi G t^2}\alpha_n(\boldsymbol{x}, \tau), \tag{28}$$

$$\boldsymbol{u}_n(\boldsymbol{r}, t) = a\boldsymbol{v}_n(\boldsymbol{x}, \tau), \tag{29}$$

$$V(\boldsymbol{r}, t) = a^2\psi(\boldsymbol{x}, \tau), \tag{30}$$

$$\boldsymbol{B}(\boldsymbol{r}, t) = B_0\boldsymbol{b}(\boldsymbol{x}, \tau), \tag{31}$$

$$\Phi(\boldsymbol{r}, t) = \pi B_0(at)^2\phi(\boldsymbol{x}, \tau), \tag{32}$$

$$M(r, t) = \frac{a^3 t}{G}m(x, \tau). \tag{33}$$

With these definitions, and with the simplifications described above, equations (14)–(24) become

$$\tau \frac{\partial \alpha_n}{\partial \tau} + (\boldsymbol{v}_n - \boldsymbol{x}) \cdot \nabla \alpha_n = 2\alpha_n - \alpha_n \nabla \cdot \boldsymbol{v}_n , \tag{34}$$

$$\tau \frac{\partial \boldsymbol{v}_n}{\partial \tau} + [(\boldsymbol{v}_n - \boldsymbol{x}) \cdot \nabla]\boldsymbol{v}_n = -\frac{1}{\alpha_n} \nabla \alpha_n - \nabla \psi - \tau^2 \frac{\mathscr{F}(\phi)}{\alpha_n} \nabla \phi , \tag{35}$$

$$\boldsymbol{v}_i = \boldsymbol{v}_n - \tau^2 \frac{\mathscr{F}(\phi)}{\chi[\alpha_n]^{3/2}} \nabla \phi , \tag{36}$$

$$\nabla^2 \psi = \alpha_n , \tag{37}$$

$$\tau \frac{\partial \phi}{\partial \tau} + 2\phi + (\boldsymbol{v}_n - \boldsymbol{x}) \cdot \nabla \phi = \tau^2 \frac{\mathscr{F}(\phi)}{\chi[\alpha_n]^{3/2}} |\nabla \phi|^2 , \tag{38}$$

where ∇ now means ∇_x and $\mathscr{F}$ is the operator defined in spherical coordinates by

$$\mathscr{F} = \frac{1}{x^2 \sin^2 \theta} \left(\frac{\partial^2}{\partial x^2} + \frac{1}{x^2} \frac{\partial^2}{\partial \theta^2} - \frac{\cot \theta}{x^2} \frac{\partial}{\partial \theta} \right) . \tag{39}$$

Notice that the dimensional parameters γ and C appear only in the nondimensional combination

$$\chi = \frac{\gamma C}{2\sqrt{\pi G}} \simeq 11.3 , \tag{40}$$

an intrinsic coupling constant representing the ratio of the time scale for ambipolar diffusion to the dynamic time scale in a magnetized cloud (see Shu 1983). The dimensionless magnetic field $\boldsymbol{b}(\boldsymbol{x}, \tau)$ now reads

$$\boldsymbol{b} = \nabla \times \boldsymbol{a} , \qquad \text{with } \boldsymbol{a} = \frac{\phi(x, \theta, \tau)}{2x \sin \theta} \hat{\boldsymbol{e}}_\varphi . \tag{41}$$

4. SEMIANALYTICAL PERTURBATIVE SOLUTION

4.1. *Validity of a Perturbative Analysis*

By construction, the initial magnetostatic equilibrium satisfies the equations of the previous section. As discussed in § 1, we are interested in a solution of the magnetic collapse problem in which the effects arising from the magnetic field are a small perturbation to the dynamical collapse of the innermost regions. Inspection of equations (34)–(38) shows that our perturbative solution must take the form of series expansions in powers of τ^2. Such a procedure will provide an approximate solution valid for $t \ll t_m$, or, equivalently, for the region $r \ll r_m$. Afterward, the perturbation approach breaks down. (Nevertheless, the small coefficients in front of many of the τ^2 terms encourage us in § 5 to apply our perturbation solution for illustrative purposes even to $\tau = 1$.) Observe that τ^2 represents also the ratio α of magnetic to thermal pressure in the initial configuration at the (unperturbed) radius of the expansion wave (see eq. [6]): $\alpha(r = at) = B_0^2/[8\pi a^2 \rho_n(at)] = \tau^2$. Therefore, a perturbative approach based on an expansion in powers of $\tau^2 \ll 1$ can be equivalently justified in the approximation of small time ($t \ll t_m$), small radius of the expansion wave ($at \ll r_m$), or small magnetic to thermal pressure ($\alpha \ll 1$).

From the discussion in § 1, we see that a perturbative analysis will give a complete description of the intermediate region in the collapse to form a *low-mass* protostar. An inner region exists, however, where the magnetic field, compressed by the infalling gas, cannot be treated as a perturbative effect. Our analysis will provide the scaling of the radius of that region with the physical parameters of the problem; it will also give the boundary conditions for the performance of a separate inner calculation in Paper II.

4.2. *Perturbation Expansion*

Following TSC we perform a series expansion in τ^2 as well as a coordinate stretching on the variable $\boldsymbol{x}$ in order to determine the deviation from spherical symmetry introduced by the magnetic field. Defining the stretched radial variable

$$y(x, \theta, \tau) = x\Delta(\theta, \tau) , \tag{42}$$

where $\Delta(\theta, \tau)$ is a function unspecified at the moment, the transformation $(\boldsymbol{x}, \tau) \equiv (x, \theta, \tau) \rightarrow (\boldsymbol{y}, \tau) \equiv (y, \theta, \tau)$ gives

$$\left(\frac{\partial}{\partial x} \right)_{\theta, \tau} = \Delta \left(\frac{\partial}{\partial y} \right)_{\theta, \tau} , \tag{43}$$

$$\left(\frac{\partial}{\partial \theta} \right)_{x, \tau} = \left(\frac{\partial}{\partial \theta} \right)_{y, \tau} + \frac{y}{\Delta} \left(\frac{\partial \Delta}{\partial \theta} \right)_{\tau} \left(\frac{\partial}{\partial y} \right)_{\theta, \tau} , \tag{44}$$

$$\left(\frac{\partial}{\partial \tau} \right)_{x, \theta} = \left(\frac{\partial}{\partial \tau} \right)_{y, \theta} + \frac{y}{\Delta} \left(\frac{\partial \Delta}{\partial \tau} \right)_{\theta} \left(\frac{\partial}{\partial y} \right)_{\theta, \tau} . \tag{45}$$

We explain all the variables in powers of τ^2, so that $A(x, \tau)$ is written

$$A(\boldsymbol{x}, \tau) = A^{(0)}(\boldsymbol{y}) + \tau^2 A^{(2)}(\boldsymbol{y}) + \mathcal{O}(\tau^4) . \tag{46}$$

The function associated with the coordinate stretching presents a special case:

$$\Delta(\theta, \tau) = 1 + \tau^2 \Delta^{(2)}(\theta) + \mathcal{O}(\tau^4) . \tag{47}$$

Substituting these expansions in the equations (34)–(38), we readily obtain a zeroth-order set of equations,

$$-2\alpha_n^{(0)} - (\boldsymbol{y} \cdot \nabla)\alpha_n^{(0)} + \nabla \cdot (\alpha_n^{(0)} \boldsymbol{v}_n^{(0)}) = 0 , \tag{48}$$

$$-(\boldsymbol{y} \cdot \nabla)\boldsymbol{v}_n^{(0)} + (\boldsymbol{v}_n^{(0)} \cdot \nabla)\boldsymbol{v}_n^{(0)} = -\frac{1}{\alpha_n^{(0)}} \nabla \alpha_n^{(0)} - \nabla \psi^{(0)} , \tag{49}$$

$$\boldsymbol{v}_i^{(0)} = \boldsymbol{v}_n^{(0)} , \tag{50}$$

$$\nabla^2 \psi^{(0)} = \alpha_n^{(0)} , \tag{51}$$

$$2\phi^{(0)} + (\boldsymbol{v}_n^{(0)} - \boldsymbol{y}) \cdot \nabla \phi^{(0)} = 0 , \tag{52}$$

and a second-order set of equations,

$$-(\boldsymbol{y} \cdot \nabla)\alpha_n^{(2)} + \nabla \cdot (\alpha_n^{(0)} \boldsymbol{v}_n^{(2)}) + \nabla \cdot (\alpha_n^{(2)} \boldsymbol{v}_n^{(0)}) = 0 , \tag{53}$$

$$2\boldsymbol{v}_n^{(2)} - (\boldsymbol{y} \cdot \nabla)\boldsymbol{v}_n^{(2)} + [(\boldsymbol{v}_n^{(0)} \cdot \nabla)\boldsymbol{v}_n^{(2)} + (\boldsymbol{v}_n^{(2)} \cdot \nabla)\boldsymbol{v}_n^{(0)}] = -\frac{1}{[\alpha_n^{(0)}]^2} (\alpha_n^{(0)} \nabla \alpha_n^{(2)} - \alpha_n^{(2)} \nabla \alpha_n^{(0)}) - \nabla \psi^{(2)} - \frac{\mathcal{F}(\phi^{(0)})}{\alpha_n^{(0)}} \nabla \phi^{(0)} , \tag{54}$$

$$\boldsymbol{v}_i^{(2)} = \boldsymbol{v}_n^{(2)} - \frac{\mathcal{F}(\phi^{(0)})}{\chi[\alpha_n^{(0)}]^{3/2}} \nabla \phi^{(0)} , \tag{55}$$

$$\nabla^2 \psi^{(2)} = \alpha_n^{(2)} , \tag{56}$$

$$4\phi^{(2)} + (\boldsymbol{v}_n^{(0)} - \boldsymbol{y}) \cdot \nabla \phi^{(2)} + \boldsymbol{v}_n^{(2)} \cdot \nabla \phi^{(0)} = \frac{\mathcal{F}(\phi^{(0)})}{\chi[\alpha_n^{(0)}]^{3/2}} |\nabla \phi^{(0)}|^2 . \tag{57}$$

To zeroth order in τ, the flow is spherically symmetric ($\Delta = 1$ and $\boldsymbol{y} = \boldsymbol{x}$). A straightforward manipulation of the equation of continuity, equations of motion, and Poisson's equation in spherical coordinates gives (Shu 1977)

$$m^{(0)} + (v_n^{(0)} - y) \frac{dm^{(0)}}{dy} = 0 , \tag{58}$$

$$[(y - v_n^{(0)})^2 - 1] \frac{dv_n^{(0)}}{dy} = \left[\alpha_n^{(0)}(y - v_n^{(0)}) - \frac{2}{y}\right](y - v_n^{(0)}) , \tag{59}$$

$$[(y - v_n^{(0)})^2 - 1] \frac{1}{\alpha_n^{(0)}} \frac{d\alpha_n^{(0)}}{dy} = \left[\alpha_n^{(0)}(y - v_n^{(0)}) - \frac{2}{y}\right](y - v_n^{(0)}) , \tag{60}$$

where the zeroth-order velocity has only a radial component $v_n^{(0)}$ and $m^{(0)}(y)$ is the reduced mass inside y,

$$m^{(0)}(y) = m^{(0)}(0) + \int_0^y \alpha_n^{(0)}(y') y'^2 \, dy' . \tag{61}$$

The governing equations therefore allow a convenient method of successive approximations, with the gas and field solved alternatively. Thus, to zeroth order in τ, since the Lorentz force does not appear in the equations of motion, the magnetic field has no effect on the collapse of the isothermal sphere. Since neutrals and ions behave as a single fluid (eq. [50]), the magnetic field is frozen in a gas that has the velocity field of the spherical nonmagnetic collapse (eq. [52]). This level of solution for the field $\boldsymbol{B}^{(0)}$ therefore reproduces the so-called *kinematic approximation*. To second order in τ, $\boldsymbol{B}^{(0)}$ is used in the set of second-order equations to evaluate the back-reaction on the flow via Lorentz force (eq. [54]) and the diffusion of the field itself (eq. [57]). The procedure can be extended, in principle, to higher orders in τ^2.

4.3. *The Zeroth-Order Magnetic Field*

The induction equation to the zeroth order, equation (52), describes the inward advection of magnetic flux along (radial) streamlines. Formally, this equation is identical to the equation for the angular momentum of TSC (their eq. [27]). In fact, a formal correspondence between angular velocity and magnetic field (and therefore between angular momentum and magnetic flux) exists in the two problems. The solution of this equation satisfying the boundary condition $\phi^{(0)}(y, \theta) = \phi_0(y, \theta) = y^2 \sin^2 \theta$ for $y \geq 1$ can be found at once by comparison vith the zeroth-order equation of continuity in the form (58) (see TSC for details), and reads

$$\phi^{(0)}(y, \theta) = \tfrac{1}{4}[m^{(0)}(y)]^2 \sin^2 \theta . \tag{62}$$

Consistent with the notation adopted in the next section, we find it convenient to write $\phi^{(0)}(y, \theta)$ in the form

$$\phi^{(0)}(y, \theta) = f^{(0)} \sin^2 \theta , \qquad \text{where } f^{(0)} = \tfrac{1}{4}[m^{(0)}(y)]^2 . \tag{63}$$

To this order, the (nondimensional) magnetic flux at the center is $\phi_c = \phi^{(0)}(0, \pi/2) = [m^{(0)}(0)]^2/4$. Restoring physical units, we discover that in the kinematic approximation the central magnetic flux Φ_c grows quadratically with time,

$$\Phi_c(t) = \frac{[m^{(0)}(0)]^2}{4} \pi B_0 a^2 t^2 , \tag{64}$$

approximately equal to one-quarter of the magnetic flux encompassed within the radius of the expansion wave.

The zeroth-order magnetic field described by the above flux function $\phi^{(0)}(y, \theta)$ is shown in Figure 2. The explicit expression for $\boldsymbol{b}^{(0)}$ is obtained from equation (41) and results in

$$\boldsymbol{b}^{(0)}(y, \theta) = \frac{[m^{(0)}(y)]^2}{4y^2} \cos \theta \hat{\boldsymbol{e}}_r - \frac{m^{(0)}(y)}{2y} \frac{dm^{(0)}}{dy} \sin \theta \hat{\boldsymbol{e}}_\theta . \tag{65}$$

Using the asymptotic formulae valid for $x \to 0$ given by Shu (1977),

$$m^{(0)} \to m^{(0)}(0) = 0.975 , \qquad \frac{dm^{(0)}}{dy} = y^2 \alpha_n^{(0)} \to \left[\frac{m^{(0)}(0)}{2}\right]^{1/2} y^{1/2} , \tag{66}$$

we see that the zeroth order magnetic field,

$$\boldsymbol{b}^{(0)}(y, \theta) \to \frac{[m^{(0)}(0)]^2}{4y^2} \cos \theta \hat{\boldsymbol{e}}_r - \left\{\frac{[m^{(0)}(0)]^3}{8y}\right\}^{1/2} \sin \theta \hat{\boldsymbol{e}}_\theta , \tag{67}$$

is asymptotically radial and diverges as y^{-2} when $y \to 0$, with the exception of a small region around the equatorial plane ($\theta = \pi/2$) where $\boldsymbol{b}^{(0)}$ is vertical and diverges as $y^{-1/2}$. There exists, in fact, a critical field line separating the magnetic field lines threading the origin from those which intersect the equatorial plane at $y > 0$. The critical field line is labeled by $f^{(0)} = [m^{(0)}(0)]^2/4$, and is described by $\cos \theta_c \simeq [2y^3/m^{(0)}(0)]^{1/4}$ for $y \to 0$. Therefore there exists a pinched equatorial zone with almost oppositely directed field lines on either side of the equatorial plane, with a vertical scale height given, for small y, by

$$h(y) = y \cos \theta_c \simeq \left[\frac{2}{m^{(0)}(0)}\right]^{1/4} y^{7/4} . \tag{68}$$

To evaluate the effects of the Lorentz force and ambipolar diffusion resulting from this configuration of the magnetic field, we need to turn to the solution of the second-order equations.

4.4. *The Second-Order Equations*

The set of second-order partial differential equations obtained in the previous section can be reduced to a set of ordinary differential equations (ODEs) by expanding the angular dependence of the physical variables in Legendre polynomials. As a

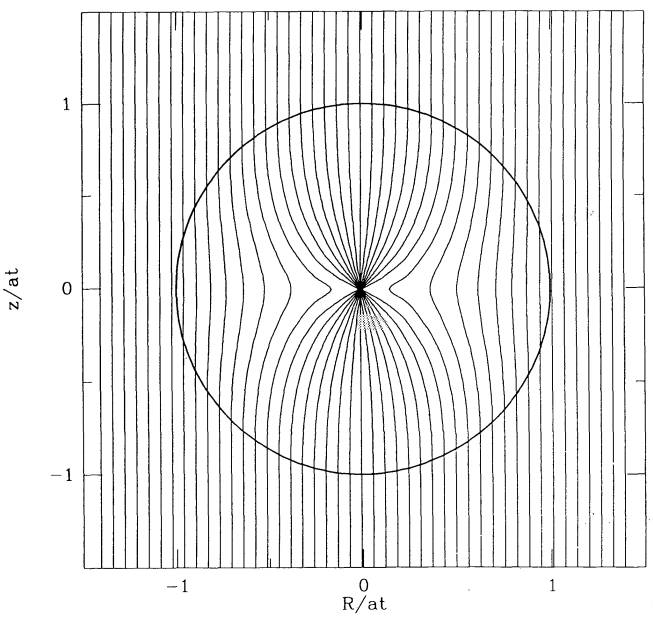

FIG. 2.—Zeroth-order self-similar solution for the magnetic field in a meridional plane. The thick circle is the head of the expansion wave.

generalization of the TSC approach, we perform here an expansion of the velocity field in *vector* spherical harmonics, obtaining the equations governing the radial part to all angular orders.

Using vector spherical harmonics $\boldsymbol{P}_J$, $\boldsymbol{B}_J$, $\boldsymbol{C}_J$, as defined by Morse & Feshbach (1953) (see Appendix B), we write

$$\boldsymbol{v}_n^{(2)}(y,\theta) = \sum_{J=0,2,\ldots} [v_J^{(2)}(y)\boldsymbol{P}_J(\theta) + w_J^{(2)}(y)\boldsymbol{B}_J(\theta)] , \tag{69}$$

$$\alpha^{(2)}(y,\theta) = \sum_{J=0,2,\ldots} \alpha_J^{(2)}(y)P_J(\theta) , \tag{70}$$

$$\psi^{(2)}(y,\theta) = \sum_{J=0,2,\ldots} \psi_J^{(2)}(y)P_J(\theta) , \tag{71}$$

$$\phi^{(2)}(y,\theta) = \sin^2\theta \sum_{J=0,2,\ldots} f_J^{(2)}(y)P_J(\theta) , \tag{72}$$

$$\Delta^{(2)}(\theta) = \sum_{J=0,2,\ldots} \Delta_J^{(2)}P_J(\theta) . \tag{73}$$

Notice in what follows that the monopole component for the tangential velocity $w_0^{(2)}$ has no physical significance since $\boldsymbol{B}_J(\theta) = 0$ for $J = 0$. The direct substitution of the above expansions into the second-order equations gives the set of ordinary differential equations for the functions describing the radial dependence of the physical quantities of the problem. We begin here with the analysis of the equation of continuity, the equation of motion, and Poisson's equation (the induction equation will be considered later). After some straightforward algebra we obtain

$$-y\frac{d\alpha_J^{(2)}}{dy} + \frac{1}{y^2}\frac{d}{dy}[y^2(\alpha^{(0)}v_J^{(2)} + \alpha_J^{(2)}v^{(0)})] - J(J+1)\frac{\alpha^{(0)}w_J^{(2)}}{y} + \Delta_J^{(2)}\left(2\alpha^{(0)} + 3y\frac{d\alpha^{(0)}}{dy}\right) = 0 , \tag{74}$$

$$2v_J^{(2)} + (v^{(0)} - y)\frac{dv_J^{(2)}}{dy} + v_J^{(2)}\frac{dv^{(0)}}{dy} = \frac{1}{[\alpha^{(0)}]^2}\left(\alpha_J^{(2)}\frac{d\alpha^{(0)}}{dy} - \alpha^{(0)}\frac{d\alpha_J^{(2)}}{dy}\right) - \frac{d\psi_J^{(2)}}{dy} + \frac{\mathscr{R}_J^{(2)}}{\alpha^{(0)}} - 3\Delta_J^{(2)}y\frac{dv^{(0)}}{dy} , \tag{75}$$

$$2w_J^{(2)} + (v^{(0)} - y)\frac{dw_J^{(2)}}{dy} + \frac{w_J^{(2)}v^{(0)}}{y} = -\frac{1}{y}\frac{\alpha_J^{(2)}}{\alpha^{(0)}} - \frac{\psi_J^{(2)}}{y} + \frac{\mathscr{T}_J^{(2)}}{\alpha^{(0)}} + \Delta_J^{(2)}(v^{(0)} - y)\frac{dv^{(0)}}{dy} , \tag{76}$$

$$\frac{1}{y^2}\frac{d}{dy}\left(y^2\frac{d\psi_J^{(2)}}{dy}\right) - \frac{J(J+1)}{y^2}\psi_J^{(2)} = \alpha_J^{(2)} + \Delta_J^{(2)}\left[J(J+1)\frac{m^{(0)}}{y^3} - 2\alpha^{(0)}\right] , \tag{77}$$

where we have dropped the subscript n in order to simplify the notation. (The density and velocity of ions and electrons can be determined a posteriori, once the equations for the neutrals have been solved). The symbols $\mathscr{R}_J^{(2)}$ and $\mathscr{T}_J^{(2)}$ represent, respectively, the coefficients of the expansion of the radial and tangential components of the Lorentz force. They both vanish for $J \geq 4$; further $\mathscr{T}_J^{(2)} = 0$ and $\mathscr{R}_J^{(2)} = -\mathscr{R}_2^{(2)}$ for $J = 0$, whereas

$$\mathscr{R}_J^{(2)} = \frac{m^{(0)}}{6y^2}\frac{dm^{(0)}}{dy}\left[\left(\frac{dm^{(0)}}{dy}\right)^2 + m^{(0)}\frac{d^2m^{(0)}}{dy^2} - \left(\frac{m^{(0)}}{y}\right)^2\right] \quad \text{for } J = 2 , \tag{78}$$

$$\mathscr{T}_J^{(2)} = \frac{(m^{(0)})^2}{12y^3}\left[\left(\frac{dm^{(0)}}{dy}\right)^2 + m^{(0)}\frac{d^2m^{(0)}}{dy^2} - \left(\frac{m^{(0)}}{y}\right)^2\right] \quad \text{for } J = 2 . \tag{79}$$

Since the inhomogeneous terms $\mathscr{R}_J^{(2)}$ and $\mathscr{T}_J^{(2)}$ vanish identically for $J \geq 4$, the null solution for $\alpha_J^{(2)}$, $v_J^{(2)}$, $w_J^{(2)}$, $\psi_J^{(2)}$, and $\Delta_J^{(2)}$ trivially satisfy the above set of ODEs for $J \geq 4$. In other words, to order τ^2, the multipole expansion for the gasdynamical variables and the gravitational potential naturally truncates after the monopole and quadrupole terms. A similar result was found by TSC for the problem when rigid rotation provides the initial second-order perturbation to the zeroth-order collapse.

The equation of continuity and the equation of motion in the radial direction can be cast in the standard form,

$$[(y - v^{(0)})^2 - 1]\frac{d\alpha_J^{(2)}}{dy} = (y - v^{(0)})\mathscr{A}_J + \alpha^{(0)}\mathscr{B}_J , \tag{80}$$

$$[(y - v^{(0)})^2 - 1]\frac{dv_J^{(2)}}{dy} = (y - v^{(0)})\mathscr{B}_J + \frac{1}{\alpha^{(0)}}\mathscr{A}_J , \tag{81}$$

where

$$\mathscr{A}_J = \frac{\alpha_J^{(2)}}{y^2}\frac{d}{dy}(y^2v^{(0)}) + \frac{v_J^{(2)}}{y^2}\frac{d}{dy}(y^2\alpha^{(0)}) - J(J+1)\frac{\alpha^{(0)}w_J^{(2)}}{y} + \Delta_J^{(2)}\left(2\alpha^{(0)} + 3y\frac{d\alpha^{(0)}}{dy}\right) , \tag{82}$$

$$\mathscr{B}_J = -\frac{\alpha_J^{(2)}}{(\alpha^{(0)})^2}\frac{d\alpha^{(0)}}{dy} + \left(2 + \frac{dv^{(0)}}{dy}\right)v_J^{(2)} + \frac{d\psi_J^{(2)}}{dy} - \frac{\mathscr{R}_J^{(2)}}{\alpha^{(0)}} + 3\Delta_J^{(2)}y\frac{dv^{(0)}}{dy} . \tag{83}$$

The vanishing of the coefficients of the derivatives on the left-hand sides of equation (80) and (81) at $y = 1$ (recall that $v^{(0)} = 0$ and $\alpha^{(0)} = 2$ at $y = 1$), clearly shows that $y = 1$ is a regular point of these equations (e.g., see Bender & Orszag 1978, § 3.1). This

singularity yields a discontinuity in the *derivatives* of the flow variables, associated with the head of an outward propagating wave. The condition of continuity for the flow variables themselves across the critical point $y = 1$ requires the right-hand side of the above equation to be zero at $y = 1$, and this gives the same constraint for both equations.

$$\mathscr{A}_J + 2\mathscr{B}_J = 0 \qquad \text{at } y = 1 . \tag{84}$$

Since the derivatives of the zeroth-order variables are not continuous across $y = 1$, the above condition gives an *internal* critical point constraint,

$$\alpha_J^{(2)}(1) + 4v_J^{(2)}(1) - J(J+1)w_J^{(2)}(1) + \frac{d\psi_J^{(2)}}{dy}(1) - \frac{\mathscr{R}_J^{(2)}(1^-)}{\alpha^{(0)}(1)} + 2\Delta_J^{(2)} = 0 \qquad \text{at } y = 1^- , \tag{85}$$

and an *external* critical point constraint,

$$\alpha_J^{(2)}(1) + 2v_J^{(2)}(1) - J(J+1)w_J^{(2)}(1) + \frac{d\psi_J^{(2)}}{dy}(1) - \frac{\mathscr{R}_J^{(2)}(1^+)}{\alpha^{(0)}(1)} - 4\Delta_J^{(2)} = 0 \qquad \text{at } y = 1^+ . \tag{86}$$

As in TSC, these two conditions are compatible only for a nonzero $\Delta_J^{(2)}$,

$$\Delta_J^{(2)} = -\frac{1}{3}\left[v_J^{(2)}(1) + \frac{\delta\mathscr{R}_J^{(2)}(1)}{4}\right], \tag{87}$$

where

$$\delta\mathscr{R}_J^{(2)}(1) = \mathscr{R}_J^{(2)}(1^+) - \mathscr{R}_J^{(2)}(1^-) . \tag{88}$$

In particular, $\delta\mathscr{R}_0^{(2)} = 8/3$, and $\delta\mathscr{R}_2^{(2)} = -8/3$. With $\Delta_J^{(2)}$ given by equation (87), the condition of smooth passage across $y = 1$ becomes

$$\alpha_J^{(2)}(1) + \frac{10}{3}v_J^{(2)}(1) - J(J+1)w_J^{(2)}(1) + \frac{d\psi_J^{(2)}}{dy}(1) = 0 . \tag{89}$$

Equation (87) yields the deviation of the head of the expansion wave from spherical symmetry. The first term in parentheses implies that the motion of the gas by itself produces a distortion of the wavefront equal to one-third the extent that the radial inflow deviates from the nonmagnetic solution, a result already found and interpreted by TSC. The second term (dominant over the first) results from the reaction of the magnetic field to the basic flow. To understand its physical meaning, we consider the relevant signal speed of the problem.

The position of the head of the expansion wave ($y = 1$) corresponds to $x = 1 - \tau^2(\Delta_0^{(2)}P_0 + \Delta_2^{(2)}P_2) + \mathscr{O}(\tau^4)$ in the x-description. By substituting equation (87) into this expression, we obtain the radius in physical units as

$$r_{\rm ew}(\theta, t) = at + \frac{at^3}{3t_m^2}\left\{\sum_{J=0,2}[v_J^{(2)}(1)P_J(\theta)] + \sin^2\theta\right\} . \tag{90}$$

By differentiating this expression with respect to t at fixed θ, we obtain the velocity of the head of the expansion wave at each θ with respect to the origin,

$$\frac{1}{a}\frac{dr_{\rm ew}}{dt} = \tau^2 \sum_{J=0,2} v_J^{(2)}(1)P_J(\theta) + (1 + \tau^2\sin^2\theta) . \tag{91}$$

The first term on the right-hand side of this equation, of second order in τ, represents simply the (nondimensional) velocity of the gas at $y = 1$ (recall that to the zeroth order in τ the velocity of the gas at the head of the expansion wave is zero), whereas the second term represents the motion of the expansion wave with respect to that gas. In an ideal magnetized gas, a disturbance can generally propagate with respect to the gas at three different phase (and group) velocities given by

$$\frac{1}{a^2}\left(\frac{\omega}{k}\right)_{\rm A}^2 = v_{\rm A}^2\cos^2\theta \tag{92}$$

for Alfvén waves, and

$$\frac{1}{a^2}\left(\frac{\omega}{k}\right)_{f,s}^2 = \frac{1 + v_{\rm A}^2 \pm \sqrt{(1+v_{\rm A}^2)^2 - 4v_{\rm A}^2\cos^2\theta}}{2} , \tag{93}$$

for fast (+) and slow (−) MHD waves. Here, $v_{\rm A}$ is the Alfvén speed in units of the sound speed a; in particular, at $r = r_{\rm ew}$,

$$a^2 v_{\rm A}(r_{\rm ew})^2 = \frac{B_0^2}{4\pi\rho(r_{\rm ew})} . \tag{94}$$

If we expand the above expressions to lowest order in τ, we obtain

$$\frac{1}{a}\left(\frac{\omega}{k}\right)_A = \frac{1}{a}\left(\frac{\omega}{k}\right)_s = \sqrt{2}\tau\cos\theta + \mathcal{O}(\tau^3)\,, \tag{95}$$

and

$$\frac{1}{a}\left(\frac{\omega}{k}\right)_f = 1 + \tau^2\sin^2\theta + \mathcal{O}(\tau^4)\,. \tag{96}$$

Comparing with equation (91) we see that, up to second order in τ, the expansion wave propagates with respect to the gas with the phase velocity of a *fast* MHD wave. In other words, the rarefaction wave in the original formulation of Shu (1977) becomes a fast MHD wave in the presence of an ordered magnetic field. This fact has an important consequence on the rate of mass accretion that will be discussed in § 5.4.

4.5. *The Induction Equation*

Let us now derive the spectral form of the induction equation. The direct substitution of the angular expansions (69)–(72) into the second-order induction equation (57) gives

$$\sum_{J=0,2,\ldots}\left\{\left[4f_J^{(2)} + (v^{(0)} - y)\frac{df_J^{(2)}}{dy} + v_J^{(2)}\frac{df^{(0)}}{dy} - \frac{\mathscr{D}_J^{(2)}}{\chi(\alpha^{(0)})^{3/2}} + 2\Delta_J^{(2)}\frac{df^{(0)}}{dy}\right]P_J + \frac{2w_J^{(2)}}{y}f^{(0)}\cot\theta\frac{dP_J}{d\theta}\right\} = 0 \tag{97}$$

where the expansion of the ambipolar diffusion term reads

$$\mathscr{D}_J^{(2)} = \begin{cases} \dfrac{1}{24}\left(\dfrac{m^{(0)}}{y}\right)^2\left[2\left(\dfrac{dm^{(0)}}{dy}\right)^2 + \left(\dfrac{m^{(0)}}{y}\right)^2\right]\left[\left(\dfrac{dm^{(0)}}{dy}\right)^2 + m^{(0)}\dfrac{d^2m^{(0)}}{dy^2} - \left(\dfrac{m^{(0)}}{y}\right)^2\right] & J = 0 \\ \dfrac{1}{12}\left(\dfrac{m^{(0)}}{y}\right)^2\left[-\left(\dfrac{dm^{(0)}}{dy}\right)^2 + \left(\dfrac{m^{(0)}}{y}\right)^2\right]\left[\left(\dfrac{dm^{(0)}}{dy}\right)^2 + m^{(0)}\dfrac{d^2m^{(0)}}{dy^2} - \left(\dfrac{m^{(0)}}{y}\right)^2\right] & J = 2 \\ 0 & J \geq 4\,. \end{cases} \tag{98}$$

The simultaneous presence of P_J and $\cot\theta\, dP_J/d\theta$ would ordinarily introduce a recurrent coupling of the various multipole orders. To discover the general form of this coupling, we express $\sin\theta$ times these functions in terms of associated Legendre polynomials with different J (e.g., see Abramowitz & Stegun 1965):

$$(2J + 1)\sin\theta P_J = P_{J+1}^1 - P_{J-1}^1\,, \tag{99}$$

$$-(2J + 1)\cos\theta\frac{dP_J}{d\theta} = (J + 1)P_{J-1}^1 + JP_{J+1}^1\,. \tag{100}$$

The independence of P_{J-1}^1 and P_{J+1}^1 now allows us to write the induction equation (97) in the spectral form:

$$\frac{1}{2J' + 1}\left[4f_{J'}^{(2)} + (v^{(0)} - y)\frac{df_{J'}^{(2)}}{dy} + v_{J'}^{(2)}\frac{df^{(0)}}{dy} + 2(J' + 1)\frac{w_{J'}^{(2)}}{y}f^{(0)} - \frac{\mathscr{D}_{J'}^{(2)}}{\chi[\alpha^{(0)}]^{3/2}} + 2\Delta_{J'}^{(2)}\frac{df^{(0)}}{dy}\right]$$
$$= \frac{1}{2J + 1}\left[4f_J^{(2)} + (v^{(0)} - y)\frac{df_J^{(2)}}{dy} + v_J^{(2)}\frac{df^{(0)}}{dy} - 2J\frac{w_J^{(2)}}{y}f^{(0)} - \frac{\mathscr{D}_J^{(2)}}{\chi(\alpha^{(0)})^{3/2}} + 2\Delta_J^{(2)}\frac{df^{(0)}}{dy}\right], \tag{101}$$

with $J' = J + 2$.

In our particular problem, $v_J^{(2)}$, $w_J^{(2)}$, $\Delta_J^{(2)}$, $\mathscr{R}_J^{(2)}$, $\mathscr{T}_J^{(2)}$, and $\mathscr{D}_J^{(2)}$ all vanish identically for $J \geq 4$. Thus, the null solution $f_J^{(2)} = 0$ constitutes a viable way to satisfy equation (101) for $J \geq 4$. Equation (97) provides a simple method to check this result. The formulae $P_0 = 1$ and $\cot\theta\, dP_2/d\theta = -(2P_2 + P_0)$ demonstrate explicitly that the bothersome term $w_J^{(2)}\cot\theta\, dP_J/d\theta$ for $J = 0, 2$ couples only to $J = 0, 2$. Higher multipole moments would be generated if we were to consider higher orders of approximation in τ, but to second order, only monopole and quadrupole corrections enter. A little algebra allows us to write the ODE for $f_J^{(2)}$ with $J = 0, 2$ as

$$4f_J^{(2)} + (v^{(0)} - y)\frac{df_J^{(2)}}{dy} + v_J^{(2)}\frac{df^{(0)}}{dy} - 2(Jw_J^{(2)} + w_{J+2}^{(2)})\frac{f^{(0)}}{y} - \frac{\mathscr{D}_J^{(2)}}{\chi(\alpha^{(0)})^{3/2}} + 2\Delta_J^{(2)}\frac{df^{(0)}}{dy} = 0\,, \tag{102}$$

where $w_4^{(2)} \equiv 0$. For compactness of notation we will continue to use the J index, although henceforth we restrict its value to 0 or 2.

4.6. *Method of Solution for the Second-Order Equations*

Having obtained the condition for a smooth transition across the critical point at the head of the expansion wave, we find it convenient to go back to the original x-description. The transformation from the y-description to the x-description can be obtained by expanding each of the physical variables, generically indicated by $g(y, \theta, \tau)$, in Taylor series up to second order in τ. Observe that

$$g(x, \theta, \tau) = g^{(0)}(y) + \tau^2 g^{(2)}(y, \theta) + \mathcal{O}(\tau^4) = \tilde{g}^{(0)}(x) + \tau^2\tilde{g}^{(2)}(x, \theta) + \mathcal{O}(\tau^4)\,, \tag{103}$$

where the tilded functions are defined by

$$\tilde{g}^{(0)}(x) \equiv [g^{(0)}(y)]_{y=x}\,, \tag{104}$$

$$\tilde{g}^{(2)}(x,\,\theta) \equiv \left[g^{(2)}(y,\,\theta) + y\,\frac{dg^{(0)}}{dy}\,\Delta^2 \right]_{y=x}\,. \tag{105}$$

Specifically, g is one of the variables α, v, w, ψ, or f; the corresponding expressions for the transformation of the corresponding radial functions is similar to equations (104)–(105).

Notice that the density and the velocity in the x-description are not continuous across $x = 1$ since the derivatives of the correspondent zeroth-order variables are not continuous at that point. The equations for the x-description are the same as those for the y-description, except that all terms proportional to $\Delta_J^{(2)}$ vanish:

$$[(x - v^{(0)})^2 - 1]\,\frac{d\tilde{\alpha}_J^{(2)}}{dx} = (x - v^{(0)})\mathscr{A}_J + \alpha^{(0)}\mathscr{B}_J\,, \tag{106}$$

$$[(x - v^{(0)})^2 - 1]\,\frac{d\tilde{v}_J^{(2)}}{dx} = (x - v^{(0)})\mathscr{B}_J + \frac{1}{\alpha^{(0)}}\,\mathscr{A}_J\,, \tag{107}$$

$$2\tilde{w}_J^{(2)} + (v^{(0)} - x)\,\frac{d\tilde{w}_J^{(2)}}{dx} + \frac{\tilde{w}_J^{(2)} v^{(0)}}{x} = \frac{1}{x}\,\frac{\tilde{\alpha}_J^{(2)}}{\alpha^{(0)}} - \frac{\tilde{\psi}_J^{(2)}}{x} + \frac{\mathscr{T}_J^{(2)}}{\alpha^{(0)}}\,, \tag{108}$$

$$\frac{1}{x^2}\,\frac{d}{dx}\left(x^2\,\frac{d\tilde{\psi}_J^{(2)}}{dx}\right) - \frac{J(J+1)}{x^2}\,\tilde{\psi}_J^{(2)} = \tilde{\alpha}_J^{(2)}\,, \tag{109}$$

$$4\tilde{f}_J^{(2)} + (v^{(0)} - x)\,\frac{d\tilde{f}_J^{(2)}}{dx} = -\tilde{v}_J^{(2)}\,\frac{df^{(0)}}{dx} + 2(J\tilde{w}_J^{(2)} + \tilde{w}_{J+2}^{(2)})\,\frac{f^{(0)}}{x} + \frac{\mathscr{D}_J^{(2)}}{\chi(\alpha^{(0)})^{3/2}}\,, \tag{110}$$

where

$$\mathscr{A}_J = \frac{\tilde{\alpha}_J^{(2)}}{x^2}\,\frac{d}{dx}\,(x^2 v^{(0)}) + \frac{\tilde{v}_J^{(2)}}{x^2}\,\frac{d}{dx}\,(x^2\alpha^{(0)}) - J(J+1)\,\frac{\alpha^{(0)}\tilde{w}_J^{(2)}}{x}\,, \tag{111}$$

$$\mathscr{B}_J = -\,\frac{\tilde{\alpha}_J^{(2)}}{(\alpha^{(0)})^2}\,\frac{d\alpha^{(0)}}{dx} + \left(2 + \frac{dv^{(0)}}{dx}\right)\tilde{v}_J^{(2)} + \frac{d\tilde{\psi}_J^{(2)}}{dx} - \frac{\mathscr{R}_J^{(2)}}{\alpha^{(0)}}\,. \tag{112}$$

Notice that the meaningless term $w_0^{(2)}$ is always multiplied by $J = 0$ when it enters as a source term for any other variable. We now turn to the solution of the equations above, beginning with the Poisson equation.

4.7. *Solution of the Poisson Equation*

The Poisson equation (109) in spectral form is a second-order ODE whose solution is well known (e.g., see Binney & Tremaine 1987, § 2.4),

$$\tilde{\psi}_J^{(2)}(x) = -\,\frac{\tilde{m}_J^{(2)}(x)}{x^{J+1}} + x^J\tilde{p}_J^{(2)}(x)\,, \tag{113}$$

where $\tilde{m}_J^{(2)}$ and $\tilde{p}_J^{(2)}$ are the moments of the density distribution inside and outside the sphere passing through the point x, defined by

$$\tilde{m}_J^{(2)}(x) = \tilde{m}_J^{(2)}(0) + \frac{1}{2J+1}\int_0^x \tilde{\alpha}_J^{(2)} x^{J+2}\,dx\,, \tag{114}$$

$$\tilde{p}_J^{(2)}(x) = \tilde{p}_J^{(2)}(\infty) + \frac{1}{2J+1}\int_x^\infty \frac{\tilde{\alpha}_J^{(2)}}{x^{J-1}}\,dx\,, \tag{115}$$

with $\tilde{m}_J^2(0)$ and $\tilde{p}_J^{(2)}(\infty)$ equal to integration constants. For future reference, the x derivative of $\tilde{\psi}_J^{(2)}$ yields

$$\frac{d\tilde{\psi}_J^{(2)}}{dx} = (J+1)\,\frac{\tilde{m}_J^{(2)}(x)}{x^{J+2}} - Jx^{J-1}\tilde{p}_J^{(2)}\,. \tag{116}$$

The condition that $\tilde{\psi}_J^{(2)}$ does not diverge as $x \to \infty$ (to recover the unperturbed equilibrium state) requires $\tilde{p}_J^{(2)}(\infty) = 0$ for every J. The term proportional to $\tilde{m}_J^{(2)}(0)$ represents the contribution to the gravitational potential of the multipole moments of the central core. In particular, if $J = 0$, equation (116) reads

$$\frac{d\tilde{\psi}_0^{(2)}}{dx} = \frac{\tilde{m}_0^{(2)}}{x^2}\,. \tag{117}$$

Observing that the transformation law (105) gives $m_0^{(2)}(0) = \tilde{m}_0^{(2)}(0)$ at $x = 0$, we conclude that $\tilde{m}_0^{(2)}(0)$ represents the mass excess (positive or negative) of the central core. To order τ^2, the quadrupole contribution of the central core is negligible compared to the contribution of the surrounding material by a line of argument similar to that given by TSC, and we set $\tilde{m}_J^{(2)}(0) = 0$ for $J = 2$.

4.8. *The External Solution* ($x > 1$)

The presence of a regular singular point in the differential equations, corresponding physically to the head of the expansion wave, requires the splitting of the solution in two parts, corresponding to $x > 1$ (the external solution) and $x < 1$ (the internal solution). The equations in the region $x > 1$, where the zeroth-order variables have their static values, have the simple forms

$$(x^2 - 1)\frac{d\tilde{\alpha}_J^{(2)}}{dx} = x\mathscr{A}_J + \frac{2}{x^2}\mathscr{B}_J , \tag{118}$$

$$(x^2 - 1)\frac{d\tilde{v}_J^{(2)}}{dx} = x\mathscr{B}_J + \frac{x^2}{2}\mathscr{A}_J , \tag{119}$$

$$2\tilde{w}_J^{(2)} - x\frac{d\tilde{w}_J^{(2)}}{dx} = -\frac{x}{2}\tilde{\alpha}_J^{(2)} + \frac{\tilde{m}_J^{(2)}}{x^{J+2}} + x^{J-1}\tilde{p}_J^{(2)} , \tag{120}$$

$$\frac{d\tilde{m}_J^{(2)}}{dx} = \frac{1}{2J+1}\tilde{\alpha}_J^{(2)}x^{J+2} , \tag{121}$$

$$\frac{d\tilde{p}_J^{(2)}}{dx} = -\frac{1}{2J+1}\frac{\tilde{\alpha}_J^{(2)}}{x^{J-1}} , \tag{122}$$

$$4\tilde{f}_J^{(2)} - x\frac{d\tilde{f}_J^{(2)}}{dx} = -2x\tilde{v}_J^{(2)} + 2x(J\tilde{w}_J^{(2)} + \tilde{w}_{J+2}^{(2)}) , \tag{123}$$

where

$$\mathscr{A}_J = -2J(J+1)\frac{\tilde{w}_J^{(2)}}{x^2} , \qquad \mathscr{B}_J = x\tilde{\alpha}_J^{(2)} + 2\tilde{v}_J^{(2)} + (J+1)\frac{\tilde{m}_J^{(2)}}{x^{J+2}} - Jx^{J-1}\tilde{p}_J^{(2)} . \tag{124}$$

Notice that $\mathscr{D}_J^{(2)} = 0$ identically for $x > 1$.

As shown in TSC, there exists only one solution of this set of homogeneous, first-order, linear ODEs, satisfying static boundary conditions at $x \to \infty$. This homogeneous solution contains an arbitrary scale factor and automatically satisfies the external critical point constraint. The continuity of the y-variables at $y = 1$ provides the condition to be satisfied by the x-variables in order to cross smoothly the critical point, namely

$$\tilde{\alpha}_J^{(2)}(1^-) + 2\Delta_J^{(2)} = \tilde{\alpha}_J^{(2)}(1^+) + 4\Delta_J^{(2)} , \tag{125}$$

$$\tilde{v}_J^{(2)}(1^-) - \Delta_J^{(2)} = \tilde{v}_J^{(2)}(1^+) , \tag{126}$$

$$\tilde{w}_J^{(2)}(1^-) = \tilde{w}_J^{(2)}(1^+) , \tag{127}$$

$$\tilde{f}_J^{(2)}(1^-) = \tilde{f}_J^{(2)}(1^+) . \tag{128}$$

These expressions give the initial values for the integration of the equations in the region $x < 1$. The scale factor is then fixed by the boundary condition on $\tilde{\psi}_J^{(2)}$ at the origin.

The homogeneous solution itself can be obtained by a series expansion in inverse even powers of x of the form

$$\tilde{m}_J^{(2)}(x) = \sum_{n=0}^{\infty}\tilde{m}_{J,2n}^{(2)}x^{-2n} , \tag{129}$$

$$\tilde{\alpha}_J^{(2)}(x) = \sum_{n=0}^{\infty}\tilde{\alpha}_{J,2n}^{(2)}x^{-2n-J-3} , \qquad \text{with } \tilde{\alpha}_{J,2n}^{(2)} = -2(2J+1)n\tilde{m}_{J,2n}^{(2)} , \tag{130}$$

$$\tilde{p}_J^{(2)}(x) = \sum_{n=0}^{\infty}\tilde{p}_{J,2n}^{(2)}x^{-2n-2J-1} , \qquad \text{with } \tilde{p}_{J,2n}^{(2)} = -\frac{2n}{2n+2J+1}\tilde{m}_{J,2n}^{(2)} , \tag{131}$$

$$\tilde{w}_J^{(2)}(x) = \sum_{n=0}^{\infty}\tilde{w}_{J,2n}^{(2)}x^{-2n-J-2} , \qquad \text{with } \tilde{w}_{J,2n}^{(2)} = (2J+1)\frac{2n^2 + n(2J+1) + 1}{(2n+J+4)(2n+2J+1)}\tilde{m}_{J,2n}^{(2)} , \tag{132}$$

$$\tilde{v}_J^{(2)}(x) = \sum_{n=0}^{\infty}\tilde{v}_{J,2n}^{(2)}x^{-2n-J-2} , \tag{133}$$

$$\tilde{f}_J^{(2)}(x) = \sum_{n=0}^{\infty}\tilde{f}_{J,2n}^{(2)}x^{-2n-J-1} , \qquad \text{with } \tilde{f}_{J,2n}^{(2)} = \frac{2}{2n+J+5}(-\tilde{v}_{J,2n}^{(2)} + J\tilde{w}_{J,2n}^{(2)} + \tilde{w}_{J+2,2n}^{(2)}) , \tag{134}$$

with $\tilde{w}_{4,2n}^{(2)} \equiv 0$ for all n.

The substitution of these formulae into the first two equations of the set gives the recurrence relations

$$\tilde{v}^{(2)}_{J,0} = -\frac{J+1}{J+4}\,\tilde{m}^{(2)}_{J,0} \qquad \text{if } n = 0\,, \tag{135}$$

$$-(2n+J+4)\tilde{v}^{(2)}_{J,2n} + (2n+J)\tilde{v}^{(2)}_{J,2n-2} = \tilde{\alpha}^{(2)}_{J,2n} + (J+1)\tilde{m}^{(2)}_{J,2n} - J\tilde{p}^{(2)}_{J,2n} - J(J+1)\tilde{w}^{(2)}_{J,2n-2} \qquad n = 1, 2, \ldots,$$

$$-(2n+J+5)\tilde{\alpha}^{(2)}_{J,2n+2} + (2n+J+1)\tilde{\alpha}^{(2)}_{J,2n} = -2J(J+1)\tilde{w}^{(2)}_{J,2n} + 4\tilde{v}^{(2)}_{J,2n} + J(J+1)\tilde{m}^{(2)}_{J,2n} - 2J\tilde{p}^{(2)}_{J,2n} \qquad n = 0, 1, 2, \ldots,$$

which define every coefficient in terms of $\tilde{m}^{(2)}_{J,0}$ (the scale factor). To determine the latter, we consider the equations for the monopole variables separately, since they are associated with the conservation of mass. Observe from equation (129) that $\tilde{m}^{(2)}_{0,0} = \tilde{m}^{(2)}_0(\infty)$, and then

$$\tilde{m}^{(2)}_0(\infty) = \tilde{m}^{(2)}_0(0) + \int_0^\infty \tilde{\alpha}^{(2)}_0 x^2\,dx = 0\,, \tag{136}$$

since whatever mass disappears from the cloud appears in the core. Therefore, $\tilde{m}^{(2)}_{0,0} = 0$ and the monopole components of all the perturbed variables vanish in the external region.

The scale factor $\tilde{m}^{(2)}_{J,0}$ for $J = 2$ cannot be determined in this way. Instead, the inward integration of the equations valid in the internal region will provide the particular value of the scale factor that yields $\tilde{m}^{(2)}_2(0) = 0$ at the origin.

4.9. *The Internal Solution* ($x < 1$)

The equations valid for $0 < x < 1$ under the boundary conditions discussed in the previous sections define a two-point boundary-value problem. The differential equations can be replaced by difference equations, which can then be solved with the relaxation method described by Press et al. (1986). Tables 1 and 2 give the resulting coefficients for the τ^2 corrections to the collapse solution. A finer examination near $x = 0$ reveals that the enhancement of the infall rate onto the central regions turns out to be negligible numerically since $\tilde{m}^{(2)}_0(0) = 4.18 \times 10^{-4}$. Except for $\tilde{f}^{(2)}_0$ and $\tilde{f}^{(2)}_2$, the multipole coefficients in Tables 1 and 2 do not depend on the numerical value of the neutral-ion coupling constant χ, as long as χ is not very small compared to unity. For $\tilde{f}^{(2)}_J$, we have decomposed the solution to equation (110) for the second-order magnetic flux function into a part $\tilde{F}^{(2)}_J$ valid for complete field freezing and another part $\tilde{D}^{(2)}_J$ arising from a correction for ambipolar diffusion:

$$\tilde{f}^{(2)}_J \equiv \tilde{F}^{(2)}_J + \frac{1}{\chi}\,\tilde{D}^{(2)}_J \qquad \text{for } J = 0, 2\,. \tag{137}$$

Figure 3 shows that when we transform to a y-description, the numerical solution of the equations for the radial functions (but not their first derivatives) for $y < 1$ attach continuously to the solution for $y > 1$, obtained as described in the previous section. To make this transformation, we use the computed coefficients describing the distortion of the head of the expansion wave: $\Delta^{(2)}_0 = -0.222$ and $\Delta^{(2)}_2 = 0.225$.

We now derive useful analytical expressions for the behavior of our semianalytical solution as $x \to 0$. For small x, we recall that the zeroth-order unperturbed solution behaves as (Shu 1977)

$$v^{(0)} \to -\left[\frac{2m^{(0)}(0)}{x}\right]^{1/2}, \qquad \alpha^{(0)} \to \left[\frac{m^{(0)}(0)}{2x^3}\right]^{1/2}, \tag{138}$$

that is, the flow approaches free-fall onto a sink of (nondimensional) mass $m^{(0)}(0)$. For the second-order solution it is convenient to consider the monopole and quadrupole component separately.

TABLE 1

MONOPOLE TERMS (EXPONENTIALS IN PARENTHESES)

x	$\tilde{\alpha}^{(2)}_0$	$\tilde{v}^{(2)}_0$	$\tilde{m}^{(2)}_0$	$\tilde{F}^{(2)}_0$	$D^{(2)}_0$
0.05.....	6.304	4.372 (−1)	8.634 (−4)	−1.130	−1.246 (1)
0.10.....	2.600	3.335 (−1)	1.959 (−3)	−3.275 (−1)	−3.168
0.15.....	1.651	2.390 (−1)	3.560 (−3)	−1.355 (−1)	−1.141
0.20.....	1.156	1.918 (−1)	5.661 (−3)	−6.415 (−2)	−5.740 (−1)
0.25.....	9.005 (−1)	1.522 (−1)	8.235 (−3)	−2.889 (−2)	−3.178 (−1)
0.30.....	7.314 (−1)	1.226 (−1)	1.130 (−2)	−8.387 (−3)	−1.878 (−1)
0.35.....	6.084 (−1)	9.579 (−2)	1.482 (−2)	5.358 (−3)	−1.049 (−1)
0.40.....	5.084 (−1)	7.103 (−2)	1.873 (−2)	1.534 (−2)	−4.547 (−2)
0.45.....	4.256 (−1)	4.828 (−2)	2.293 (−2)	2.303 (−2)	3.393 (−4)
0.50.....	3.517 (−1)	2.640 (−2)	2.730 (−2)	2.931 (−2)	3.924 (−2)
0.55.....	2.829 (−1)	5.058 (−3)	3.166 (−2)	3.454 (−2)	7.431 (−2)
0.60.....	2.172 (−1)	−1.588 (−2)	3.579 (−2)	3.888 (−2)	1.070 (−1)
0.65.....	1.488 (−1)	−3.791 (−2)	3.935 (−2)	4.225 (−2)	1.376 (−1)
0.70.....	8.091 (−2)	−5.975 (−2)	4.196 (−2)	4.442 (−2)	1.650 (−1)
0.75.....	8.360 (−3)	−8.293 (−2)	4.312 (−2)	4.504 (−2)	1.867 (−1)
0.80.....	−6.836 (−2)	−1.071 (−1)	4.221 (−2)	4.358 (−2)	1.992 (−1)
0.85.....	−1.512 (−1)	−1.330 (−1)	3.847 (−2)	3.935 (−2)	1.966 (−1)
0.90.....	−2.406 (−1)	−1.605 (−1)	3.097 (−2)	3.146 (−2)	1.708 (−1)
0.95.....	−3.382 (−1)	−1.902 (−1)	1.859 (−2)	1.881 (−2)	1.103 (−1)
1.00.....	−4.444 (−1)	−2.222 (−1)	0.0	0.0	0.0

TABLE 2

QUADRUPOLE TERMS (EXPONENTIALS IN PARENTHESES)

x	$\tilde{\alpha}_2^{(2)}$	$\tilde{v}_2^{(2)}$	$\tilde{w}_2^{(2)}$	$\tilde{m}_2^{(2)}$	$\tilde{p}_2^{(2)}$	$F_2^{(2)}$	$D_2^{(2)}$
0.05.....	−1.096 (3)	−2.581	−2.085	−3.860 (−5)	−7.539 (1)	−2.253	−2.484 (1)
0.10.....	−1.191 (2)	−1.533	−4.890	−1.541 (−4)	−7.275	−6.517 (−1)	−6.258
0.15.....	−3.148 (1)	−8.072 (−1)	−1.811	−3.044 (−4)	−1.730	−2.722 (−1)	−2.221
0.20.....	−1.158 (1)	−5.666 (−1)	−8.842 (−1)	−4.847 (−4)	−5.586 (−1)	−1.345 (−1)	−1.102
0.25.....	−5.105	−3.905 (−1)	−4.816 (−1)	−6.831 (−4)	−1.999 (−1)	−6.993 (−2)	−6.127 (−1)
0.30.....	−2.456	−2.790 (−1)	−2.807 (−1)	−8.874 (−4)	−6.591 (−2)	−3.593 (−2)	−3.645 (−1)
0.35.....	−1.217	−1.928 (−1)	−1.628 (−1)	−1.083 (−3)	−1.062 (−2)	−1.660 (−2)	−2.213 (−1)
0.40.....	−5.889 (−1)	−1.254 (−1)	−8.779 (−2)	−1.253 (−3)	1.294 (−2)	−5.864 (−3)	−1.297 (−1)
0.45.....	−2.569 (−1)	−7.156 (−2)	−3.852 (−2)	−1.385 (−3)	2.267 (−2)	−6.809 (−4)	−7.020 (−2)
0.50.....	−7.024 (−2)	−2.614 (−2)	−4.481 (−3)	−1.462 (−3)	2.600 (−2)	8.213 (−4)	−1.112 (−2)
0.55.....	3.790 (−2)	1.267 (−2)	1.928 (−2)	−1.470 (−3)	2.625 (−2)	−3.086 (−4)	−2.139 (−3)
0.60.....	1.042 (−1)	4.650 (−2)	3.578 (−2)	−1.389 (−3)	2.500 (−2)	−3.338 (−3)	−1.615 (−2)
0.65.....	1.505 (−1)	7.724 (−2)	4.683 (−2)	−1.191 (−3)	2.294 (−2)	−7.681 (−3)	2.744 (−2)
0.70.....	1.845 (−1)	1.042 (−1)	5.306 (−2)	−8.405 (−4)	2.046 (−2)	−1.272 (−2)	3.252 (−2)
0.75.....	2.163 (−1)	1.288 (−1)	5.512 (−2)	−2.841 (−4)	1.769 (−2)	−1.778 (−2)	3.269 (−2)
0.80.....	2.492 (−1)	1.510 (−1)	5.312 (−2)	5.579 (−4)	1.469 (−2)	−2.191 (−2)	2.839 (−2)
0.85.....	2.865 (−1)	1.711 (−1)	4.704 (−2)	1.800 (−3)	1.146 (−2)	−2.392 (−2)	2.104 (−2)
0.90.....	3.302 (−1)	1.889 (−1)	3.670 (−2)	3.609 (−3)	7.941 (−3)	−2.219 (−2)	1.199 (−2)
0.95.....	3.823 (−1)	2.045 (−1)	2.179 (−2)	6.218 (−3)	4.102 (−3)	−1.457 (−2)	3.732 (−3)
1.00.....	4.437 (−1)	2.177 (−1)	1.898 (−3)	9.951 (−3)	−1.214 (−4)	1.729 (−3)	0.0

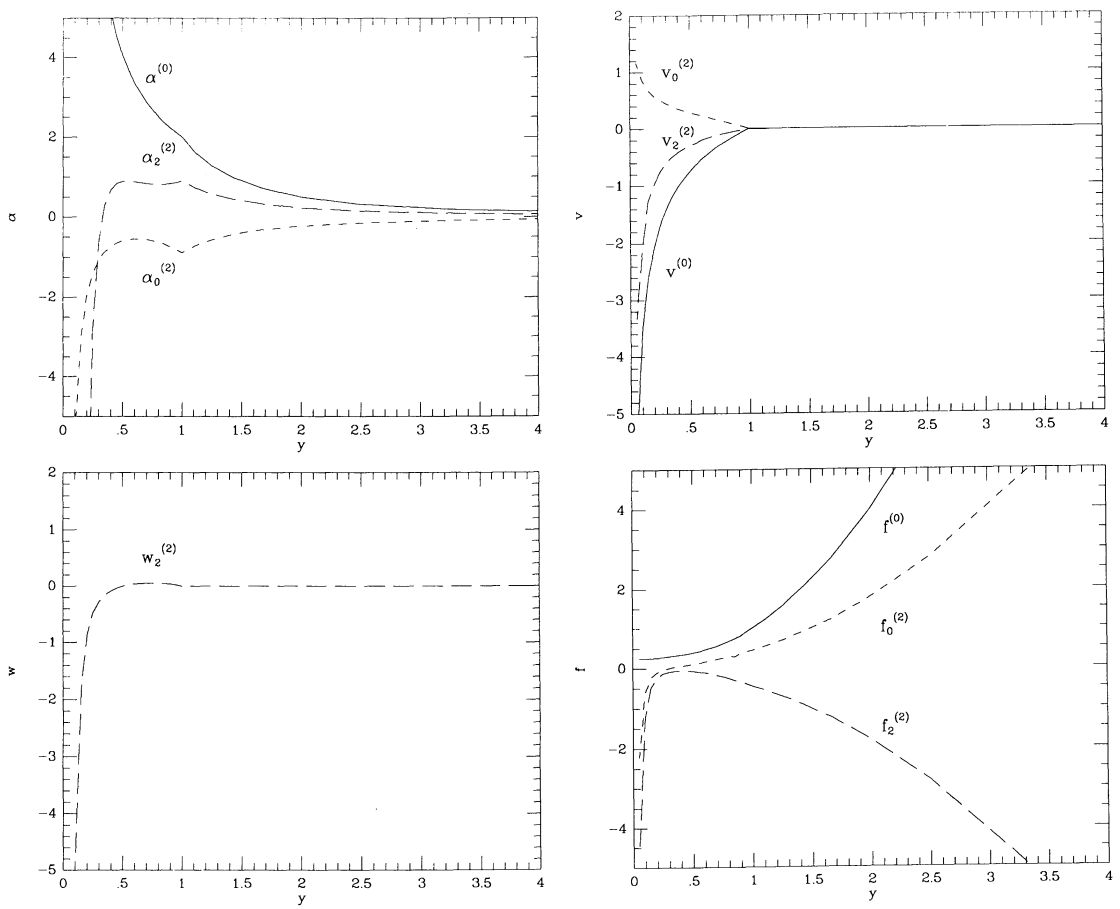

FIG. 3.—Zeroth- and second-order (untilded) variables α_J (density), v_J (radial velocity), w_J (tangential velocity), and f_J (magnetic flux) as functions of the stretched radial coordinate y, for $J = 0, 2$ and $\chi = 11.3$. Notice that there are no monopole components for w. The point $y = 1$ identifies the head of the expansion wave, across which the physical variables are continuous but their first derivatives are not. For $y < 1$ the second-order variables (denoted by the superscript 2) are obtained by numerical solution of the second-order equations, whereas for $y > 1$ the solutions have the analytical series solution described in the text (truncated after the 1000th term).

4.9.1. *Monopole Variables*

After some straightforward but tedious algebra, we obtain for the monopole components of the perturbation in the density and in the velocity as $x \to 0$

$$\tilde{\alpha}_0^{(2)} \to \frac{[m^{(0)}(0)]^3 + 6\tilde{m}_0^{(2)}(0)}{12[2m^{(0)}(0)]^{1/2}} x^{-3/2} \tag{139}$$

and

$$\tilde{v}_0^{(2)} \to \frac{[m^{(0)}(0)]^3 - 6\tilde{m}_0^{(2)}(0)}{6[2m^{(0)}(0)]^{1/2}} x^{-1/2} . \tag{140}$$

The monopole component of the magnetic flux function obeys

$$\tilde{f}_0^{(2)} \to -\frac{[m^{(0)}(0)]^{9/2}}{36\sqrt{2}} x^{-3/2} - \frac{1}{54\chi} \{2[m^{(0)}(0)]^{19}\}^{1/4} x^{-9/4} , \tag{141}$$

whereas the monopole component of the Lorentz acceleration and the ambipolar diffusion coefficient respectively behave as

$$\tau^2 \frac{1}{\alpha^{(0)}} \mathscr{R}_0^{(2)} \to \frac{1}{6} \tau^2 [m^{(0)}(0)]^3 x^{-2} , \tag{142}$$

and

$$\mathscr{D}_0^{(2)} \to -\tfrac{1}{24}[m^{(0)}(0)]^6 x^{-6} . \tag{143}$$

4.9.2. *Quadrupole Variables*

In an analogous way, a straightforward algebraic analysis of the equations to the quadrupole order shows that, as $x \to 0$,

$$\tilde{\alpha}_2^{(2)} \to -\tfrac{1}{6}[m^{(0)}(0)]^3 x^{-3} , \tag{144}$$

$$\tilde{v}_2^{(2)} \to -\tfrac{1}{6}[m^{(0)}(0)]^2 x^{-1} , \tag{145}$$

and

$$\tilde{w}_2^{(2)} \to -\tfrac{1}{12}[m^{(0)}(0)]^3 x^{-2} . \tag{146}$$

The quadrupole component of the magnetic flux function asymptotically becomes

$$\tilde{f}_2^{(2)} \to -\frac{[m^{(0)}(0)]^{9/2}}{18\sqrt{2}} x^{-3/2} - \frac{1}{27\chi} \{2[m^{(0)}(0)]^{19}\}^{1/4} x^{-9/4} . \tag{147}$$

Notice that $\tilde{f}_2^{(2)} \to 2\tilde{f}_0^{(2)}$ for $x \to 0$; this result implies that the angular dependence of the second-order correction to the magnetic flux ϕ equals $\sin^2\theta \cos^2\theta$ and reaches a maximum somewhat above and below the equatorial plane, with the consequences that will be discussed in § 5.5 and Paper II. In the same limit for small x, the components of the Lorentz force in the radial and tangential directions read

$$\tau^2 \frac{1}{\alpha^{(0)}} \mathscr{R}_0^{(2)} \to -\frac{1}{6} \tau^2 [m^{(0)}(0)]^3 x^{-2} , \tag{148}$$

$$\tau^2 \frac{1}{\alpha^{(0)}} \mathscr{T}_2^{(2)} \frac{dP_2}{d\theta} \to \frac{1}{4} \tau^2 \{2[m^{(0)}(0)]^7\}^{1/2} x^{-7/2} \cos\theta \sin\theta . \tag{149}$$

Finally, the quadrupole ambipolar diffusion coefficient, for small x, is

$$\mathscr{D}_2^{(2)} \to -\tfrac{1}{12}[m^{(0)}(0)]^6 x^{-6} . \tag{150}$$

5. RESULTS AND DISCUSSION

5.1. *An Evolutionary Sequence*

As a graphical example, Figures 4*a* and 4*b* and 5*a* and 5*b* show the semianalytical solution complete to second order in τ for our standard choices of parameter values, where we have plotted density contours, magnetic field lines, and arrows representing the flow velocity. The two snapshots of the collapse are taken at times $\tau = 0.4$ and 0.8, corresponding to $t = 1.1 \times 10^5$ and 2.3×10^5 yr, respectively. The shape of the head of the expansion wave (indicated by the heavy solid curve) makes clear that the collapse propagates in the cloud as a fast MHD wave, traveling *faster* (as a magnetosonic wave) in the direction *perpendicular* to the magnetic field than (as an acoustic wave) parallel to it. This situation yields a result contrary to the usually envisaged picture of collapse being retarded in the direction perpendicular to the field lines. Indeed, the first few density contours immediately inside the head of the expansion wave show actually a *prolate*, instead of an oblate, shape. Deeper inside, the tangential component of the

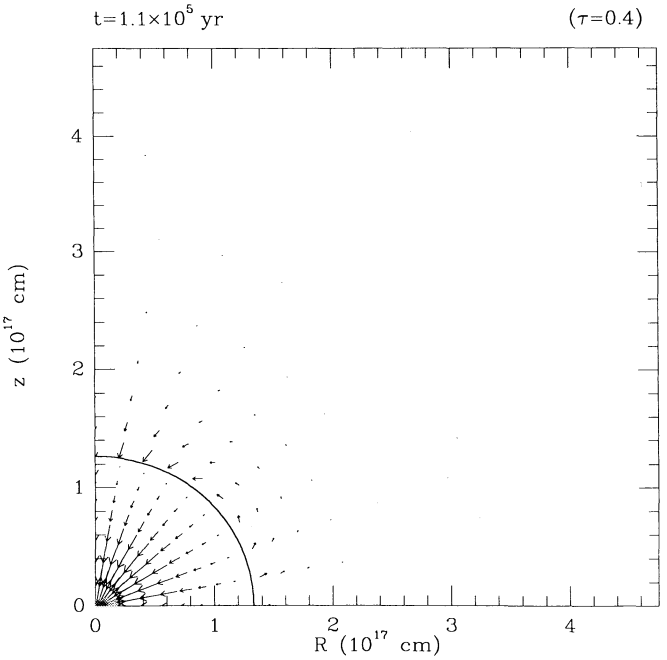

FIG. 4a

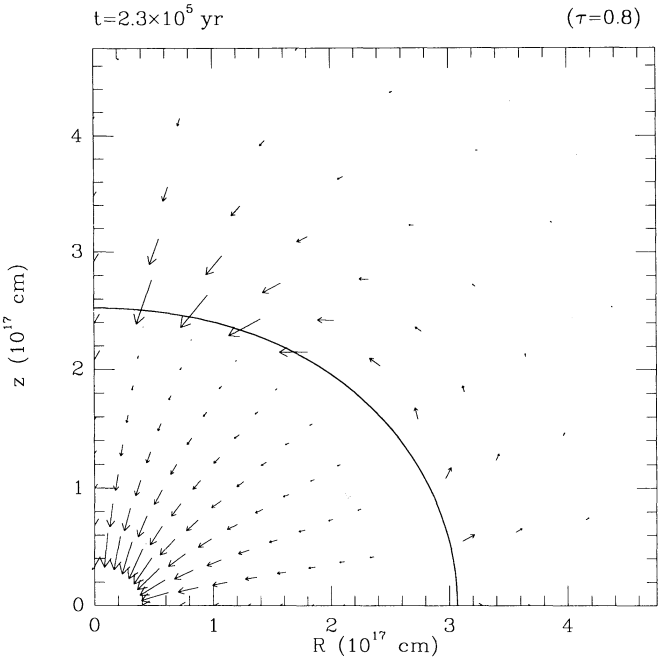

FIG. 4b

FIG. 4.—Velocity field in a meridional plane at two times, corresponding to (*a*) $\tau = 0.4$ and (*b*) $\tau = 0.8$, calculated according to the solutions plotted in Fig. 3. The magnitude of the velocity outside the expansion wave has been increased by a factor 1000. The thick line marks the head of the expansion wave. The velocity scale is such that one small division in the R or θ scale corresponds to 0.30 km s^{-1} in the region inside the expansion wave, and to 30 cm s^{-1} outside the expansion wave.

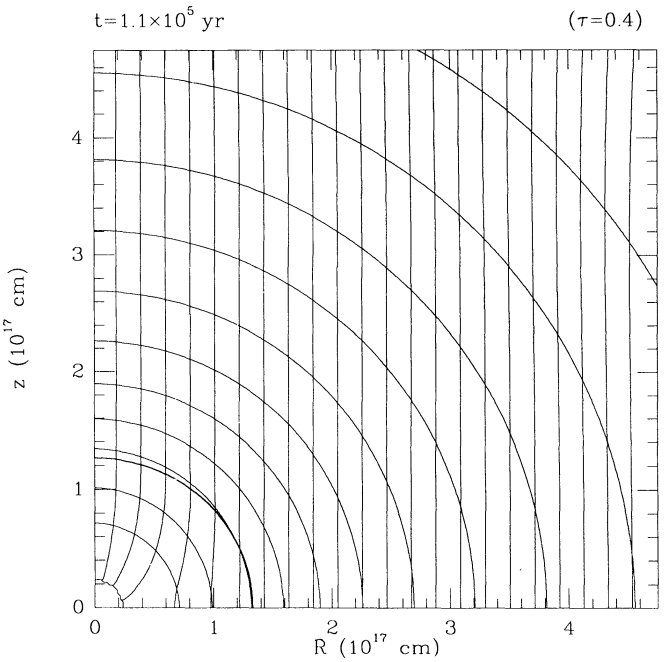

FIG. 5a

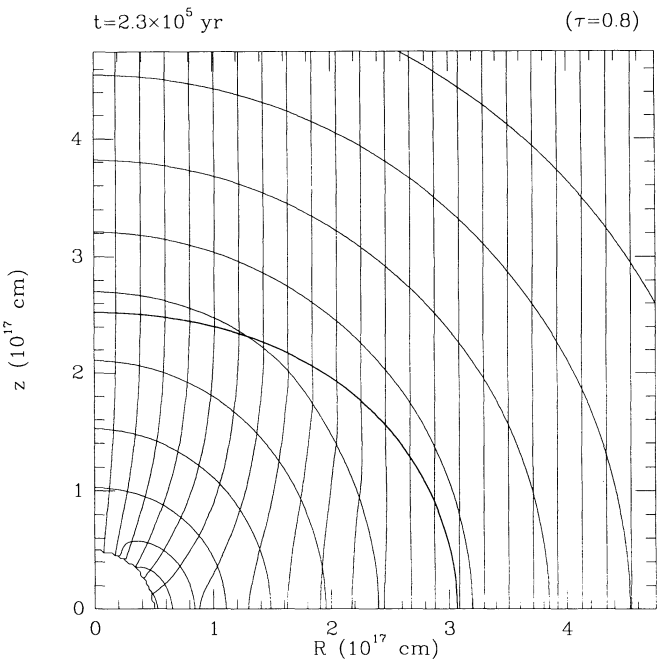

FIG. 5b

FIG. 5.—Density contours and magnetic field lines in a meridional plane at the same times as in Fig. 4, calculated according to the solutions plotted in Fig. 3. The thick line marks the head of the expansion wave. Density contours are drawn for values of the density increasing by a factor $\sqrt{2}$, starting from 1×10^{-20} g cm^{-3} at the most external contour. The density and the magnetic field lines have been clipped at $x = 0.2$; inside this radius the semianalytical solution begins to break down and has been excluded. The mass accreted on the central protostar at these two times is equal to 1.1 and 2.3 $M_\odot$, the accretion rate being 1.0×10^{-5} $M_\odot$ yr^{-1}.

Lorentz force produced by the curvature of the magnetic field lines deflects the gas toward the equatorial plane, forming the oblate circumstellar distribution of material evident in Figure 4*b*.

The perturbative method described in this paper cannot follow the propagation of the magneto-expansion wave into the magnetically dominated envelope of the cloud (the region $r > r_m$), but we stress again that for our standard choice of the physical parameters the mass involved in the collapse is of the order of $6\,M_\odot$ when the head of the expansion wave reaches $r = r_m$. This by itself makes unlikely the explanation for the masses of protostars offered by Mouschovias (1976b) on the basis of magnetic support of the envelopes of equilibrium models. Moreover, in the case of the collapse of a supercritical cloud, Scott & Black (1980) found (even with helpful boundary conditions) that only a small fraction of the outer envelope of a collapsing cloud, of order 10% or less of the total mass, is prevented from collapsing by the tension of the magnetic field lines, so that the effect, which probably does occur to some extent for $r > r_m$ (see below), may not be as decisive as supposed by Mouschovias. In any case, an extension of the present study to the collapse of the outer regions of an unbounded cloud would be quite interesting.

The velocity field plotted in Figures 4*a* and 4*b* shows an increasing growth (with time, and with decreasing distance from the center) of magnetic pinch-forces directed toward the equatorial plane (see Mestel 1966; Mestel & Strittmatter 1967; Mestel 1969). Outside the magneto-expansion wave, the velocity is generated by the gravitational quadrupole moment of the pseudodisk mass distribution; the values of the velocity are very small there (less than 1% of the sound speed) and decrease rapidly (as r^{-4}) to zero at large r. On the other hand, inside the expansion wave, the velocity increases monotonically with decreasing radius from zero to supersonic values. The latter behavior differs markedly from that found by Mouschovias & Morton (1991, 1992a, b) in models of the contraction of long cylindrical clouds, where the velocity usually decreases from supersonic (and sometimes supermagnetosonic) values at the cloud boundary to zero at the cloud center. The difference is susceptible to observational test in the line profiles of molecular transitions in dense cores. Indeed, the results of Zhou et al. (1990, 1992) and Zhou (1992) mentioned in § 1 may already have eliminated the latter type of behavior in isolated cores and Bok globules.

5.2. *Magnetic "Pinch" Forces*

From equations (139)–(140) we see that for small x the monopole second-order density and velocity have the same radial dependence as the corresponding zeroth-order variables. This is consistent with the asymptotic behavior of the monopole term in the expression for the Lorentz acceleration, equation (142), which has clearly the same dependence on x as the zeroth-order gravitational acceleration produced by the protostar. The monopole component of the total (Newton + Lorentz) acceleration as $x \to 0$ is then

$$a^{\rm mon} = -\frac{d\psi^{(0)}}{dx} - \tau^2\left(\frac{d\tilde{\psi}_0^{(2)}}{dx} - \frac{\mathscr{R}_0^{(2)}}{\alpha^{(0)}}\right) \to -\frac{m^{(0)}(0) + \tau^2\tilde{m}_0^{(2)}(0)}{x^2} + \tau^2\frac{[m^{(0)}(0)]^3}{6x^2}\,, \tag{151}$$

and the monopole velocity to lowest order in τ asymptotically reads

$$v^{\rm mon} \to -\sqrt{2\,|\,a^{\rm mon}\,|\,x} \to -[2m^{(0)}(0)]^{1/2}x^{-1/2} + \tau^2\frac{[m^{(0)}(0)]^3 - 6\tilde{m}_0^{(2)}(0)}{6[2m^{(0)}(0)]^{1/2}}\,x^{-1/2}\,, \tag{152}$$

in agreement with equation (140). The similar x dependences of the various contributions to the monopole component of the solution imply that the magnetic forces effectively produce a simple "dilution" of the gravitational forces that lead asymptotically to free-fall collapse. According to our perturbative analysis, the dilution factor for the monopole density and velocity has the time-dependent form $1 + \tau^2[c_0(x)P_0(\theta) + c_2(x)P_2(\theta)] + \mathcal{O}(\tau^4)$, with the $c_J(x)$ approaching constant values as $x \to 0$.

The quadrupole component of the Lorentz acceleration in the radial direction, equation (148), being proportional to x^{-2} for small x, also does not introduce deviation from a magnetically diluted gravitational collapse, and the total Lorentz acceleration is given asymptotically by

$$\tau^2\frac{1}{\alpha^{(0)}(x)}[\mathscr{R}_0^{(2)}(x)P_0(\theta) + \mathscr{R}_2^{(2)}(x)P_2(\theta)] \to \tau^2\frac{[m^{(0)}(0)]^2}{4x^2}\sin^2\theta\,, \tag{153}$$

which is zero at the pole, $\sin\theta = 0$, and has a maximum magnitude at the equator $\sin\theta = 1$. Since the coefficient multiplying $x^{-2}\sin^2\theta$ in the expression (153) is smaller than the same coefficient in the expression for the gravitational force (by a factor $\approx\tau^2 m^{(0)}(0)/4$), our perturbative analysis consistently predicts that the tension of the magnetic field lines in the radial direction cannot overtake gravity as $x \to 0$ for fixed τ smaller than unity. Because the anisotropic dilution suffered by the radial gravitational collapse increases quadratically with dimensionless time τ (to leading order), a naive extrapolation to $\tau > 1$ misleadingly suggests that magnetic decelerations might reverse the equatorial flow after the expansion wave has propagated into the magnetically dominated envelope of the cloud ($r_{\rm ew} > r_m$). In practice, the linear perturbative solution breaks down before this happens, and the more reliable nonlinear calculations of Paper II give no indication of such a process occurring around $\tau \approx 1$. The smallness of the coefficient $m_0^{(2)}(0)$ yields another indication that mass infall at essentially the standard rate continues well beyond the nominal point $\tau = 1$, unless it is somehow terminated by other means (e.g., a stellar wind).

The quadrupole solution introduces a more important effect. As we mentioned before, the dominant effect of the Lorentz force on the dynamics of the accretion flow is to produce a component of the velocity in the tangential direction that asymptotically dominates the radial component (eq. [146]). This "magnetic pinch effect" is clearly shown by the asymptotic behavior of the Lorentz acceleration in the tangential direction, which increases as $x^{-7/2}$, faster than the radial component, as $x \to 0$ (eq. [149]). This "pinching" force is responsible for the progressive flattening of the density distribution around the protostar (formation of a "pseudodisk") and eventually the detachment of part of the magnetic field from that of the background (see Paper II). Other

workers arrived at opposing positions on this controversial point on the basis of equilibrium studies. Our dynamical result agrees with the view of Mestel (1966) and Mestel & Strittmatter (1967), but conflicts with that expressed by Mouschovias (1976b), according to whom no equatorial pinching forces appear during the contraction of a cloud and the magnetic field of the cloud never detaches from the background.

5.3. *Radius of the "Pseudodisk"*

The origin of the "pseudodisk" resides in the magnetic pinching forces that deflect infalling fluid elements toward the equatorial plane. Despite apparent similarities, this situation is qualitatively (and quantitatively) different from the collapse of a rotating isothermal sphere, where the initial angular velocity of the cloud is responsible for the retardation of the flow and the formation of a centrifugally *supported* circumstellar disk. Moreover, for typical rotation rates of molecular clouds, the head of the expansion wave is very slightly *prolate* in the direction of the angular velocity vector of the cloud (TSC). However, as in the problem of rotating collapse, it is possible to obtain *analytically* the scaling of the size of the region where the dynamics is dominated by non-gravitational forces. In the case of an initial uniform rotation Ω_0 of the cloud, for instance, simple considerations of angular momentum conservation applied to Shu's (1977) spherical collapse (TSC) give the scaling of the *centrifugal* radius r_C as

$$r_C = k_C a \Omega_0^2 t^3 , \tag{154}$$

where k_C is a nondimensional numerical constant. In analogy with r_C, we can define a "magnetic radius" r_B determining the size of the region of influence of magnetic fields near the protostar. We obtain the scaling of r_B by equating the perturbation in the meridional velocity (generated by the Lorentz force) to the asymptotic free-fall collapse velocity. Since the tangential component of the perturbed velocity ($w \propto \tau^2 x^{-2}$) increases faster with decreasing x than the radial component ($v \propto x^{-1/2}$) the Lorentz force formally overtakes gravity inside a radius whose scaling is given by the condition $x^{-1/2} \propto \tau^2 x^{-2}$. In physical variables, this implies

$$r_B = k_B \left(\frac{G^2 B_0^4}{a} \right)^{1/3} t^{7/3} , \tag{155}$$

where k_B is a nondimensional numerical constant. The above expressions for r_C and r_B are strictly valid only in the limit of small time. The nondimensional constants k_C and k_B cannot be determined from the perturbative solution for the intermediate region; one has to have a valid solution for the inner regions. In the nonmagnetic but rotating case, solutions in closed form exist for the latter problem (Cassen & Moosman 1981), so the value of $k_C = [m^{(0)}(0)]^3/16 \simeq 0.058$ can be obtained analytically. Lorentz forces are more complex than inertial forces, so one has to perform a numerical integration of the differential equations for the inner problem to obtain k_B (see Paper II). Both cases are examples of intermediate asymptotics (Barenblatt 1979), where a nondimensional constant appears when one modifies an original problem possessing a self-similar solution (the spherical collapse of the singular isothermal sphere) by introducing additional effects (rotation or magnetic fields) that remove the degeneracy of the problem and make the self-similarity of the solution incomplete.

5.4. *The Infall Rate*

As we have seen, the coefficient to τ^2 in the enhancement of the mass infall rate onto the central regions $\tilde{m}_0^{(2)}(0) = 4.18 \times 10^{-4}$ is numerically very small. This important fact implies that for all practical purposes we recover the infall rate appropriate for the nonmagnetic case, $\dot{M} = m^{(0)}(0) a^3/G$, where $m^{(0)}(0) = 0.975$. The result has a physical interpretation that clarifies the subtle role of magnetic fields in a dynamical calculation. In order to understand what factors control the mass infall rate, consider the total amount of mass (in nondimensional units) that crosses per unit time an ideal sphere of radius x around the origin

$$m(x, \tau) = -\tfrac{1}{2} x^2 \int_0^{\pi/2} \alpha_n(\boldsymbol{x}, \tau) \boldsymbol{v}_n(\boldsymbol{x}, \tau) \cdot \hat{\boldsymbol{e}}_x \sin\theta \, d\theta . \tag{156}$$

Inserting the expansions of density and velocity in this expression and integrating over θ, it is obvious that the quadrupole variables bring no contribution, and to the lowest order in τ the accretion rate reads

$$m(x, \tau) = -x^2 \alpha^{(0)}(x) v^{(0)}(x) - \tau^2 x^2 [\alpha^{(0)}(x) \tilde{v}_0^{(2)}(x) + v^{(0)}(x) \tilde{\alpha}_0^{(2)}(x)] . \tag{157}$$

This expression shows that the mass accretion rate in the nonmagnetic collapse (first term on the right-hand side) is modified by the (ordered) magnetic field by the two terms in the brackets. These corrections contain the perturbation in the density and in the radial velocity, respectively. The two terms have opposite sign and comparable magnitude, and as $x \to 0$ they nearly cancel each other, leaving a net contribution numerically equal to $\tilde{m}_0^{(2)}(0) = 4.18 \times 10^{-4}$. Thus, two competing effects control the mass accretion rate in our problem, *both* having their origin in the magnetic field: the first is the *reduction* of the infall velocity produced by the Lorentz force (for small x, $\tilde{v}_0^{(2)}$ is directed *outward*, its value depending on the magnetic field strength and ambipolar diffusion through the solution of the monopole equations); the second is the *increase* of the mass of the cloud that is collapsing at a given time with respect to the nonmagnetic solution, as expressed by the monopole component of the density (for small x, $\tilde{\alpha}_0^{(2)}$ is *positive*) and produced by the increase in the speed of propagation of the collapse (the expansion wave, being a fast MHD wave, engulfs more gas at a given time than the corresponding nonmagnetic sonic expansion wave). The collapse of the cloud is *both* retarded and propagated faster—the cause being the very same for both effects, namely the amount of distortion of the original magnetic field—with the contributions being of almost equal but opposite strengths. This result conflicts with the magnetically controlled accretion rate found by Mouschovias & Morton (1992b), smaller than the corresponding nonmagnetic accretion rate by the ratio of the ambipolar diffusion to the free-fall time scale. But their conclusion applies to a situation where the system does not exist in all aspects fully in

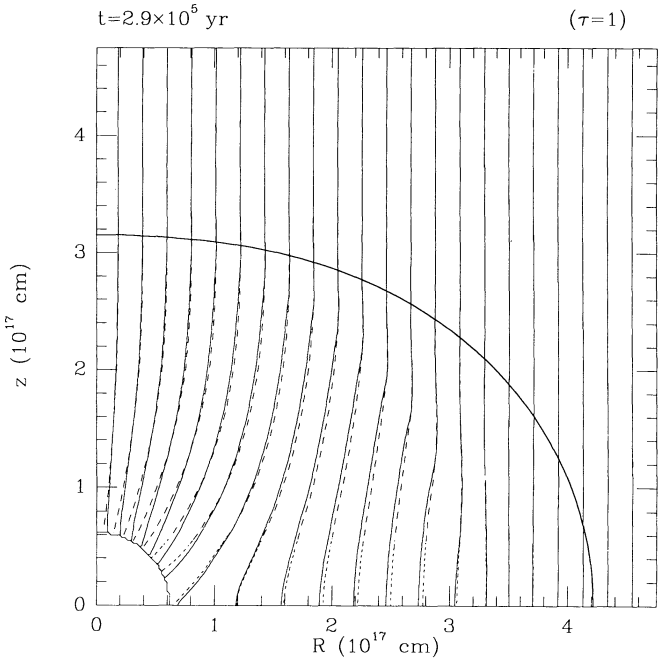

FIG. 6.—Magnetic field lines for $\tau = 1$ (*solid lines*) compared with the magnetic field lines obtained without ambipolar diffusion (*dashed lines*)

dynamical collapse. A reduction of the standard infall rate by (at least) the factor 14.7 recommended by these authors in all circumstances would pose serious difficulties for the statistics of embedded versus revealed sources (Kenyon & Hartmann 1990) as well as for the interpretation of the birthline in the H-R diagram for pre–main-sequence stars (Palla & Stahler 1992).

5.5. *The Magnetic Flux*

Figure 6 shows the effects of ambipolar diffusion on the magnetic field at $\tau = 1$ (when the perturbation expansion to only quadratic order begins to give exaggerated results). The magnetic field has been left behind in the inner regions with respect to the magnetic field obtained under field-freezing conditions, the effect being larger in the innermost parts. Ambipolar diffusion does not, however, "drag out" the magnetic field everywhere. The motion of field lines relative to neutrals is driven by the Lorentz force, which opposes collapse only in the innermost region. Behind the head of the expansion wave, where the Lorentz force slightly compresses the gas producing prolate density contours, the magnetic field is dragged slightly "in" rather than "out" by ambipolar diffusion.

The asymptotic behavior of the magnetic flux function is given by equations (141) and (147). The first terms in the expansions for $\tilde{f}_0^{(2)}$ and $\tilde{f}_2^{(2)}$, $\propto x^{-3/2}$, represent the reduction in the inflow of magnetic flux into the central regions produced by the magnetic deflection of the otherwise radial infall toward the midplane of a pseudodisk. These corrections amount to a large effect at small x, but they arise for purely dynamical reasons and would hold even under conditions of complete field freezing. The effect by itself therefore does not resolve the classical problem of the eventual decrease of the magnetic flux during gravitational collapse. The latter requires field diffusion or dissipation.

The diffusion of magnetic field due to ion-neutral drift is given in equations (141) and (147) by terms inversely proportional to χ. After multiplying them by the corresponding angular functions and summing over $J = 0, 2$, we find that the second-order distortion of the magnetic field produced by ambipolar diffusion diverges strongly as $\tau^2 x^{-9/4} \sin^2\theta \cos^2\theta$ when $x \to 0$. In other words, ambipolar diffusion does not allow the progressive stretching of the magnetic field lines with decreasing distance from the center found in § 4.3. The modification produced by ambipolar diffusion in that configuration takes the form of a perturbation growing with time and with decreasing distance from the center, with a maximum above and below the equatorial plane and asymptotically vanishing on it. We believe that this is the beginning, to a perturbative level, of a process that leads ultimately to the formation of a neutral line and to a change of the topology of the magnetic field configuration through the intervention of ohmic dissipation. This point will be analyzed in more detail in Paper II. The issue, of course, cannot be studied in our perturbative approach, since the divergence of the second-order variables with respect to the zeroth-order ones invalidates the perturbative solution for small x. In fact, from the condition $\tau^2 \tilde{f}_0^{(2)} \simeq f^{(0)}$ we get $x_p \simeq 0.2\tau^{4/3}$ for $\chi \gg 1$ as an estimate of the reduced radius inside which the perturbative approach begins to break down. Because of this, in Paper II we will present a numerical solution of the MHD equations, obtained under the appropriate simplifying hypotheses valid for $x < x_p$, that will enable us to follow the nonlinear evolution of the features we have highlighted in the analysis presented here.

This work was funded in part by NSF grant AST-9024260 and in part under the auspices of a special NASA Astrophysics Theory Program that supports a joint center for Star Formation Studies at NASA/Ames Research Center, the University of California at Berkeley, and the University of California at Santa Cruz.

APPENDIX A

NONDIMENSIONAL PARAMETERS, LENGTH SCALES, AND TIME SCALES

In a general formulation, the relevant physical quantities that enter in the problem of formation, evolution, and collapse of self-gravitating, isothermal molecular cloud cores are a typical size ℓ, a typical neutral density ρ_n, a typical magnetic field strength B, the effective sound speed a, the gravitational constant G, and the product of the friction drag coefficient γ with the proportionality constant C of the ρ_i-ρ_n relation, defined in the text. The dimensions of these quantities are $[\ell] = L$, $[\rho_n] = ML^{-3}$, $[B] = M^{1/2}L^{-1/2}T^{-1}$, $[a] = LT^{-1}$, $[G] = M^{-1}L^3T^{-2}$, and $[\gamma C] = M^{-k}L^{3k}T^{-1}$, where k is the exponent in the ρ_i-ρ_n relation. Simple dimensional analysis shows that the above dimensional quantities introduce in the problem four independent nondimensional parameters, four independent length scales, and three independent time scales. A particular (physically meaningful) choice is the following (Fiedler & Mouschovias 1992, with their notation):

1. The nondimensional parameters k, $\alpha \sim B^2/(a^2\rho_n)$, $\mu \sim \ell\rho_n\sqrt{G}/B$, and $v_{\rm ff} \sim \gamma C\rho_n^{k-1/2}/\sqrt{G}$;
2. The physical length scale ℓ, the length scale for damping of Alfvèn waves $\lambda_{\rm A} \sim B/(\gamma C\rho_n^{k+1/2})$, the critical length scale for thermal support $\lambda_{T,{\rm cr}} \sim a/\sqrt{G\rho_n}$, and the critical length scale for magnetic support $\lambda_{M,{\rm cr}} \sim B/(\rho_n\sqrt{G})$;
3. The free-fall time scale $\tau_{\rm ff} \sim 1/\sqrt{G\rho_n}$, the ion-neutral collision time scale $\tau_{\rm ni} \sim 1/(\gamma C\rho_n^k)$, and the sound crossing time scale $\tau_s \sim \ell/a$.

The physical meaning of these quantities has been discussed by Mouschovias (1991a, b). The space of solutions of the problem of magnetic collapse varies in three spatial dimensions and time and is controlled by the four nondimensional parameters defined above. Even if we restrict the geometry to infinite cylindrical symmetry (one nonignorable spatial coordinate), a thorough exploration of the space of solutions presents a rather lengthy task, as the parametric study of Mouschovias and Morton (1991, 1992a, b) shows.

Conceptual and practical advantages can be obtained by dividing the general problem into different stages (see Shu et al. 1987). The detailed analysis by LS, for instance, emphasized the governing nondimensional parameters of the phase of the *formation* of molecular cloud cores as k, $v_{\rm ff}$, and the product $\alpha\mu$ (called $l\mathscr{R}$ by them), plus a fourth nondimensional parameter introduced by turbulent pressure. Notice that the combination $\alpha\mu$ is independent on the density, as well as $v_{\rm ff}$ for $k = \frac{1}{2}$. In their study, the first three parameters were kept fixed at their "canonical" values while the fourth was varied within reasonable limits and the large value of the square of $v_{\rm ff}$ was used to justify a quasi-static treatment of the momentum equation (see Shu 1983). By the end of the quasi-static phase, molecular cloud cores entering the phase of *dynamical collapse* have acquired power-law density profiles over a significant spatial range. Since there is no characteristic density nor characteristic size in such a core (if isolated), ℓ and ρ_n disappear from the list of characteristic dimensional quantities. As a consequence, only one (relevant) nondimensional parameter, $\gamma CB^{2k-1}/(\sqrt{G}\,a^{2k-1})$ is left to control the subsequent evolution of the core; for $k = \frac{1}{2}$ this is our χ, identical to Fiedler & Mouschovias's (1992) $v_{\rm ff}$. This parameter represents essentially the ratio (independent of density, if $k = \frac{1}{2}$) of the free-fall and neutral-ion collision times; its "canonical" numerical value is of the order of 10 (11.3 with our values, 8.31 according to Mouschovias 1991c).

The relevant length scales and time scales, if $k = \frac{1}{2}$, reduce to $a^2/(B\sqrt{G})$ and $a/(B\sqrt{G})$; apart from a factor 2, they are our r_m and t_m, respectively. The length scale r_m yields a critical (not a typical) length scale of equivalent physical significance as the critical mass-to-flux ratio (see § 1). Our initial configuration, for instance, has $(M/\Phi)_{\rm cr} \geq 1$ for $r \leq r_m/(2c)$ (see § 2.2). Thus, our definition of r_m essentially replaces Fiedler & Mouschovias's (1992) definition of $\lambda_{M,{\rm cr}}$. No other length or time or mass scale enters our problem by a priori considerations to define, for example, the mass of the forming star.

APPENDIX B

VECTOR SPHERICAL HARMONICS

We give here the explicit expressions for the vector spherical harmonics adopted in the present work in terms of the polar basis $\hat{\boldsymbol{e}}_r, \hat{\boldsymbol{e}}_\theta, \hat{\boldsymbol{e}}_\varphi$. Different conventions and normalizations are possible; we have followed Morse & Feshbach (1953) by defining

$$\boldsymbol{P}_J^M = [P_J^M(\theta, \phi), 0, 0]\,, \tag{158}$$

$$\boldsymbol{B}_J^M = \left[0, \frac{\partial P_J^M}{\partial\theta}(\theta, \phi), \frac{1}{\sin\theta}\frac{\partial P_J^M}{\partial\phi}(\theta, \phi)\right], \tag{159}$$

$$\boldsymbol{C}_J^M = \left[0, -\frac{1}{\sin\theta}\frac{\partial P_J^M}{\partial\phi}(\theta, \phi), \frac{\partial P_J^M}{\partial\theta}(\theta, \phi)\right]. \tag{160}$$

In the text, whenever the index M is omitted, it is intended $M = 0$ (axial symmetry).

REFERENCES

Abramowitz, M., & Stegun, I. A. 1965, Handbook of Mathematical Functions (New York: Dover)
Adams, F. C., & Shu, F. H. 1986, ApJ, 308, 836
Adams, F. C., Lada, C. J., & Shu, F. H. 1987, ApJ, 312, 788
———. 1988, ApJ, 326, 865
Barenblatt, G. I. 1979, Similarity, Self-Similarity, and Intermediate Asymptotics (New York: Consultants Bureau)
Bender, C. M., & Orszag, S. A. 1978, Advanced Mathematical Methods for Scientists and Engineers (New York: McGraw-Hill)
Binney, J., & Tremaine, S. 1987, Galactic Dynamics (Princeton: Princeton Univ. Press), 62
Black, D. C., & Scott, E. H. 1982, ApJ, 263, 696
Butner, H. M., Evans, N. J., Lester, D. F., Levrault, R. M., & Strom, S. E. 1991, ApJ, 376, 636
Carr, J. S. 1987, ApJ, 323, 170
Cassen, P., & Moosman, A. 1981, Icarus, 48, 353
Dalgarno, A., Oppenheimer, M., & Berry, R. S. 1973, ApJ, 183, L21
Dorfi, E. 1982, A&A, 114, 151
Draine, B. T., Roberge, W. G., & Dalgarno, A. 1983, ApJ, 264, 485
Dudurov, A. E. 1988, in Magnetic Stars, ed. Yu. V. Glagolevski & J. M. Kopylov (Leningrad: Nauka), 226
———. 1990, in Galactic and Intergalactic Magnetic Fields, ed. R. Beck, P. P. Kronberg, & R. Wielebinski (Dordrecht: Reidel), 189
Elmegreen B. G. 1979, ApJ, 232, 729
El-Nawawy, M. S., Aiad, A., & El-shalaby, M. A. 1988, MNRAS, 232, 809
El-Nawawy, M. S., Ateya, B. G., & Aiad, A. 1992, Ap&SS, 190, 257
Evans, N. J. 1991, in Frontiers of Stellar Evolution, ed. D. L. Lambert (San Francisco: ASP), 45
Falgarone, E., & Pérault, M. 1987, in Physical Processes in Interstellar Clouds, ed. G. E. Morfill & M. Scholer (Dordrecht: Reidel), 59
Fiedler, R. A., & Mouschovias, T. C. 1992, ApJ, 391, 219
Heiles, C., Goodman, A., McKee, C. F., & Zweibel, E. G. 1993, in Protostars and Planets III, ed. M. S. Matthews & E. Levy (Tucson: Univ. Arizona Press), 279
Kenyon, S. J., & Hartmann, L. W. 1990, ApJ, 349, 197
Lada, C. J. 1991, in The Physics of Star Formation and Early Stellar Evolution, ed. C. J. Lada & N. D. Kylafis (Dordrecht: Kluwer), 329
Langer, W. D. 1985, in Protostars and Planets III, ed. D. C. Black & M. S. Matthews (Tucson: Univ. Arizona Press), 650
Lizano, S., & Shu, F. H. 1989, ApJ, 342, 834 (LS)
Loren, R. B. 1989, ApJ, 338, 925
McKee, C. F., Zweibel, E., Goodman, A. A., & Heiles, C. 1993, in Protostars and Planets III, ed. M. S. Matthews & E. Levy (Tucson: Univ. Arizona Press), 327
Mestel, L. 1965, QJRAS, 6, 161
———. 1966, MNRAS, 133, 265
———. 1969, in Plasma Instabilities in Astrophysics, ed. D. A. Tidman & D. G. Wentzel (New York: Gordon & Breach), 329
———. 1985, in Protostars and Planets II, ed. D. C. Black & M. S. Matthews (Tucson: Univ. Arizona Press), 320
Mestel, L., & Spitzer, L. 1956, MNRAS, 116, 505
Mestel, L., & Strittmatter, P. A. 1967, MNRAS, 137, 95
Morse, P. M., & Feshbach, H. 1953, Methods of Theoretical Physics (New York: McGraw-Hill)
Mouschovias, T. Ch. 1976a, ApJ, 206, 753
———. 1976b, ApJ, 207, 141
———. 1987a, in Physical Processes in Interstellar Clouds, ed. G. E. Morfill & M. Scholer (Dordrecht: Reidel), 453
Mouschovias, T. Ch. 1987b, in Physical Processes in Interstellar Clouds, ed. G. E. Morfill & M. Scholer (Dordrecht: Reidel), 491
———. 1991a, in The Physics of Star Formation and Early Stellar Evolution, ed. C. J. Lada & N. D. Kylafis (Dordrecht: Kluwer), 61
———. 1991b, in The Physics of Star Formation and Early Stellar Evolution, ed. C. J. Lada & N. D. Kylafis (Dordrecht: Kluwer), 449
Mouschovias, T. Ch., & Morton, S. A. 1991, ApJ, 371, 296
———. 1992a, ApJ, 390, 144
———. 1992b, ApJ, 390, 166
Mouschovias, T. Ch., Paleologou, E. V., & Fiedler, R. A. 1985, ApJ, 291, 772
Mouschovias, T. Ch., & Spitzer, L. 1976, ApJ, 210, 326
Myers, P. C., Fuller, G. A., Goodman, A. A., & Benson, P. J. 1991, ApJ, 376, 561
Nakano, T. 1976, PASJ, 28, 355
———. 1979, PASJ, 31, 697
———. 1981, Prog. Theor. Phys. Suppl., 70, 54
———. 1984, Fund. Cosmic Phys., 9, 139
———. 1988, in Galactic and Extragalactic Star Formation, ed. R. E. Pudritz & M. Fich (Dordrecht: Kluwer), 111
———. 1992, in Young Star Clusters and Early Stellar Evolution, a special issue of Mem. Soc. Astron. Italiana, in press
Nakano, T., & Umebayashi, T. 1986, MNRAS. 218. 663
Natta, A., Palla, F., Butner, H. M., Evans, N., & Harvey, P. M. 1992, ApJ, 391, 805
Nishi, R., Nakano, T., & Umebayashi, T. 1991, ApJ, 368, 181
Oppenheimer, M., & Dalgarno, A. 1974, ApJ, 192, 29
Paleologou, E. V., & Mouschovias, T. Ch. 1983, ApJ, 275, 838
Palla, F., & Stahler, S. 1992, ApJ, 392, 667
Phillips, G. J. 1986a, MNRAS, 221, 571
———. 1986b, MNRAS, 222, 111
Phillips, G. J., & Monaghan, J. J. 1985, MNRAS, 216, 883
Press, W. H., Flannery, B. P., Teukolsky, S. A., & Vetterling, W. T. 1986, Numerical Recipes (Cambridge: Cambridge Univ. Press)
Scott, E. H., & Black, D. C. 1980, ApJ, 239, 166
Shu, F. H. 1977, ApJ, 214, 488
———. 1983, ApJ, 273, 202
Shu, F. H., Adams, F., & Lizano, S. 1987, ARA&A, 25, 23
Shu, F. H., Najita, J., Galli, D., Ostriker, E., & Lizano, S. 1993, in Protostars and Planets III, ed. M. S. Matthews & E. Levy (Tucson: Univ. Arizona Press), 3
Spitzer, L. 1968, in Stars and Stellar Systems, vol. 8, ed. B. M. Middlefurst & L. H. Aller (Chicago: Univ. Chicago Press)
Terebye, S., Shu, F. H., & Cassen, P. 1984, ApJ, 286, 529 (TSC)
Tomisaka, K. 1991, ApJ, 376, 190
Tomisaka, K., Ikeuchi, S., & Nakamura, T. 1988a, ApJ, 326, 208
———. 1988b, ApJ, 335, 239
———. 1989, ApJ, 341, 220
———. 1990, ApJ, 362, 202
Umebayashi, T. 1983, Progr. Theor. Phys., 69, 480
Umebayashi, T., & Nakano, T. 1980, PASJ, 22, 405
———. 1990, MNRAS, 243, 103
Whitney, B. A., & Hartmann, L. W. 1992, ApJ, 359, 529
Zhou, S. 1992, ApJ, 394, 204
Zhou, S., Evans, N. J., Butner, H. M., Kutner, M. L., Leung, C. M., & Mundy, L. G. 1990, ApJ, 363, 168
Zhou, S., Evans, N. J., Kömpe, C., & Walmsley, M. 1992, preprint